Autorità di Bacino Distrettuale dell' Appennino Meridionale

Terzo Focus dedicato all'approfondimento
30 settembre 2021

Nuove frontiere dell'idrologia per una maggiore sicurezza dei territori

Mauro Fiorentino

Università degli Studi della Basilicata

Presidente del Gruppo Italiano di Idraulica
Presidente del CINID, Consorzio Interuniversitario per l'Idrologia

Le alluvioni: rischio e protezione


PATRICK DENNIS/AP


Flood

Flood occurrence in the world 1985-2010

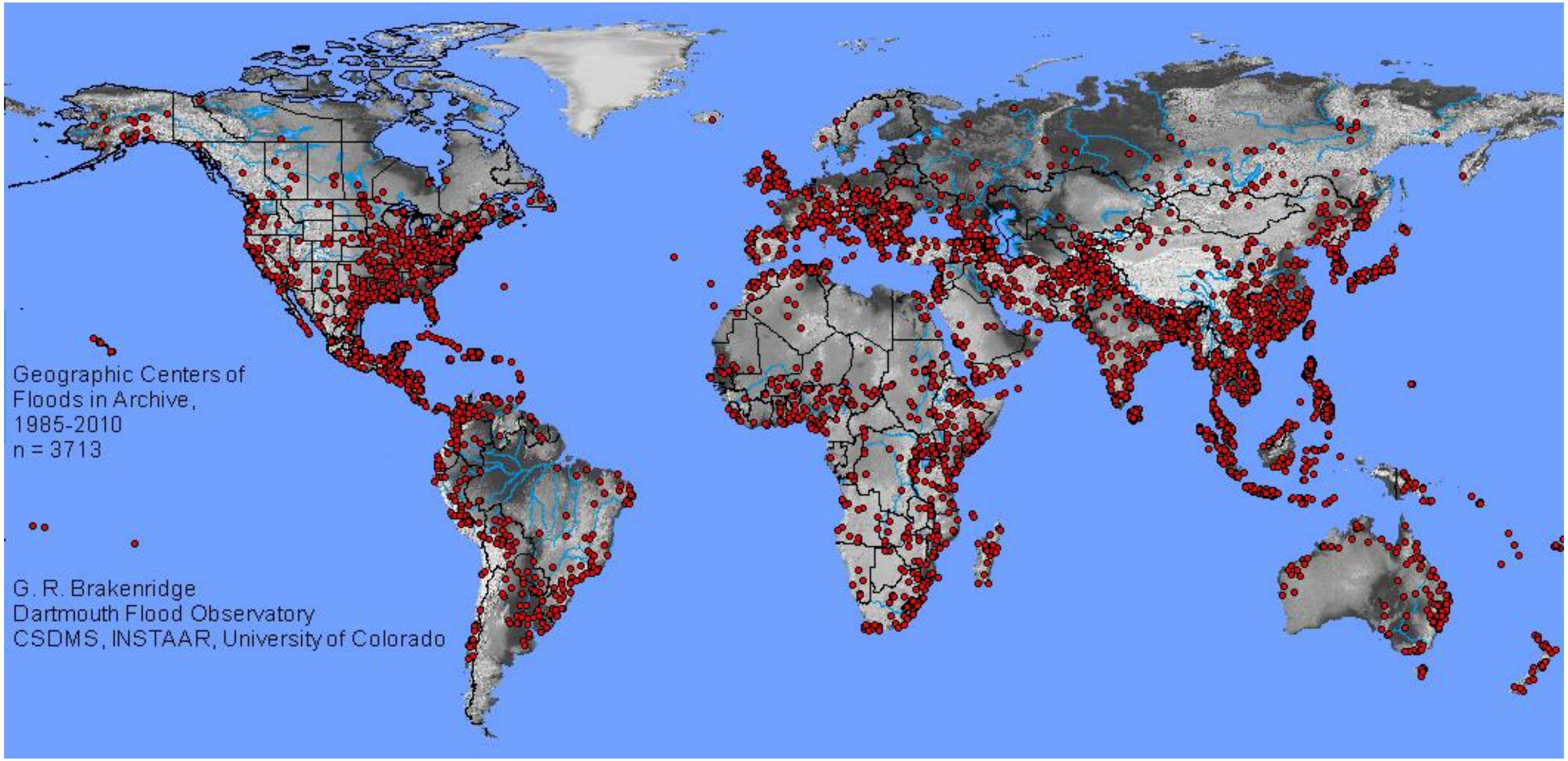

G.R.Brakenridge, "Global Active Archive of Large Flood Events", Dartmouth Flood Observatory, University of Colorado, http://floodobservatory.colorado.edu/Archives/index.html.

THE HUMAN COST OF NATURAL DISASTERS 2015

A global perspective

Centre for Research on the Epidemiology of Disasters
CRED

UCL Université catholique de Louvain

Institute of Health and Society (IRSS)

USAID FROM THE AMERICAN PEOPLE

UNISDR The United Nations Office for Disaster Risk Reduction

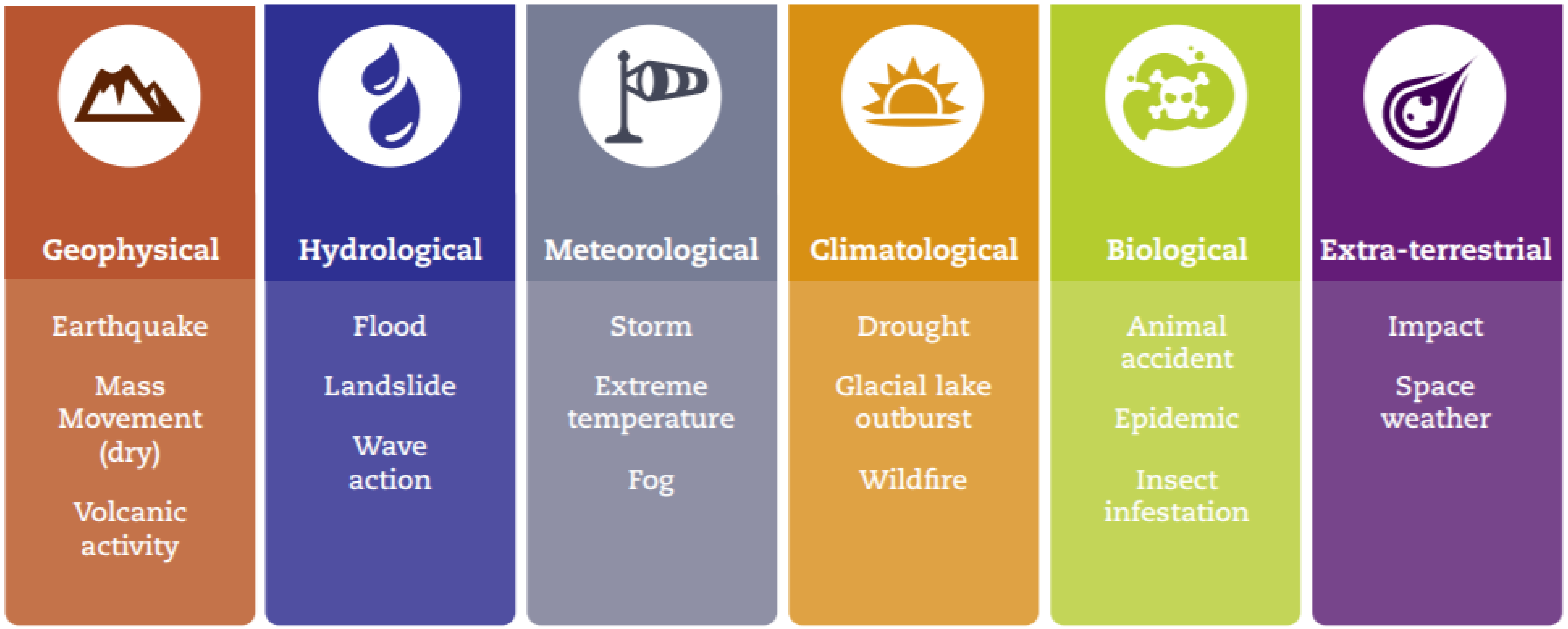
Geophysical
Earthquake
Mass Movement (dry)
Volcanic activity
Hydrological
Flood
Landslide
Wave action
Meteorological
Storm
Extreme temperature
Fog
Climatological
Drought
Glacial lake outburst
Wildfire
Biological
Animal accident
Epidemic
Insect infestation
Extra-terrestrial
Impact
Space weather

Share of occurrence of natural disasters by disaster type (1994-2013)

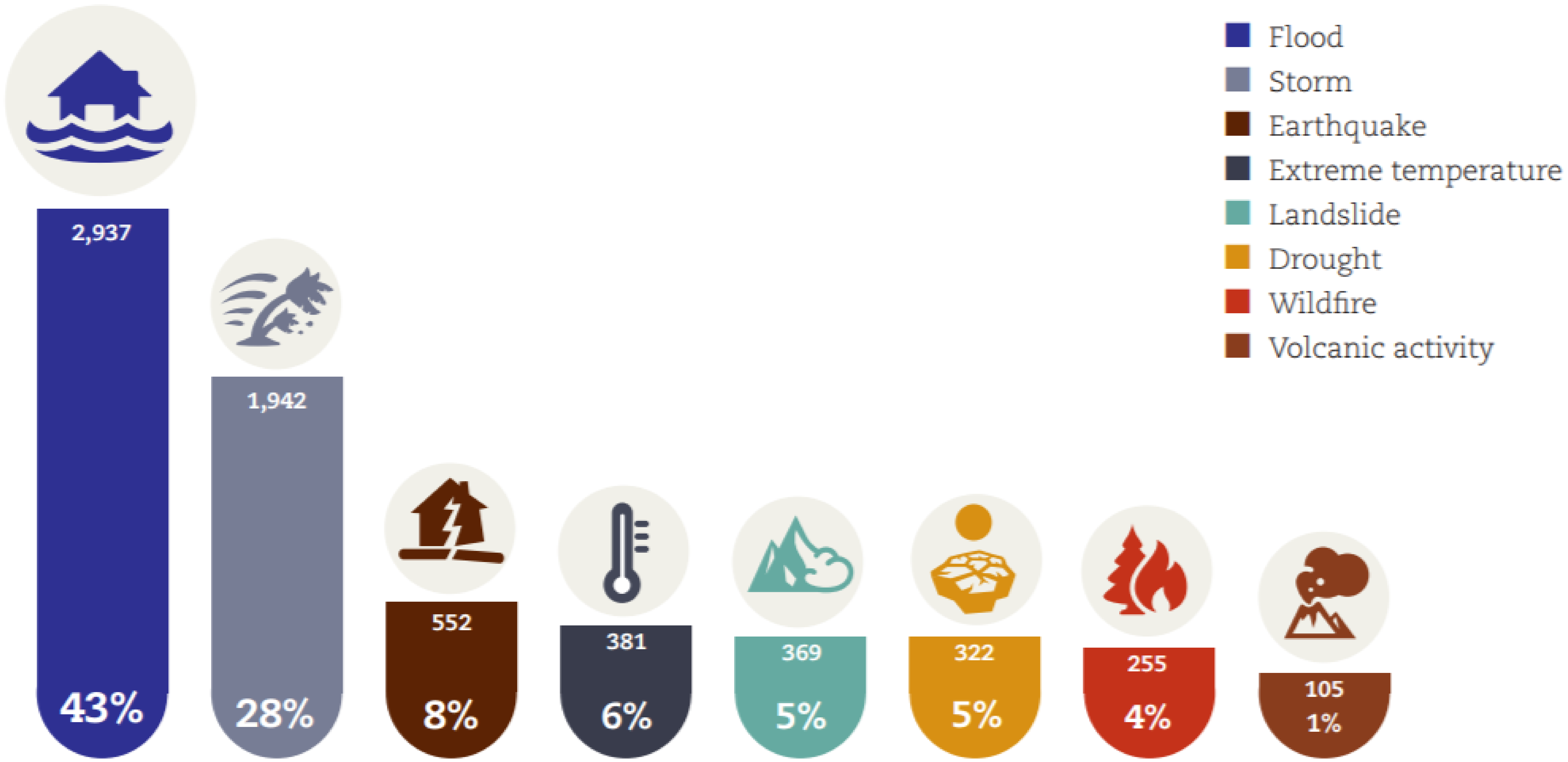

Number of people affected by disaster type (1994-2013)
(NB: deaths are excluded from the total affected)

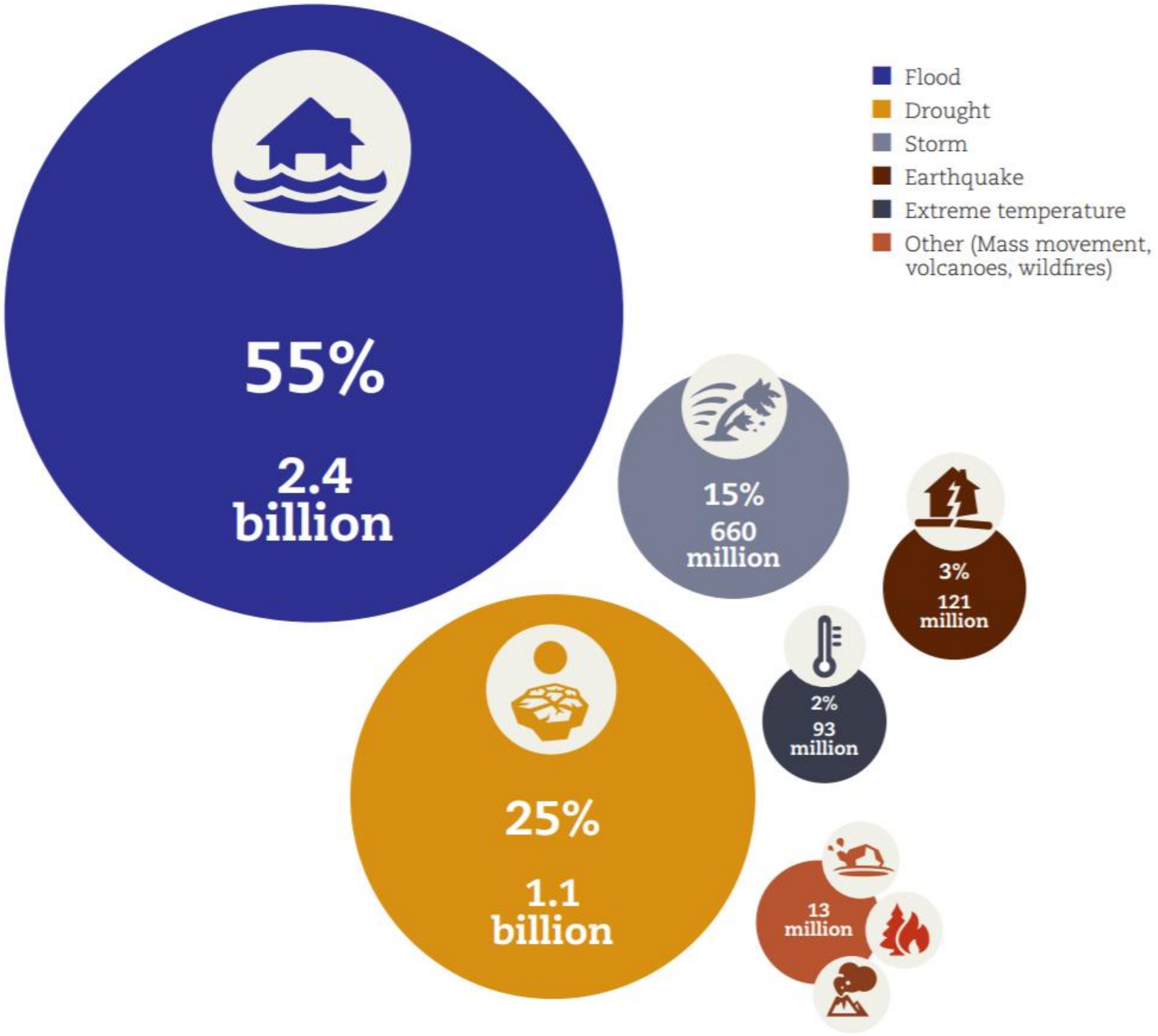

Number of deaths by disaster type (1994-2013)

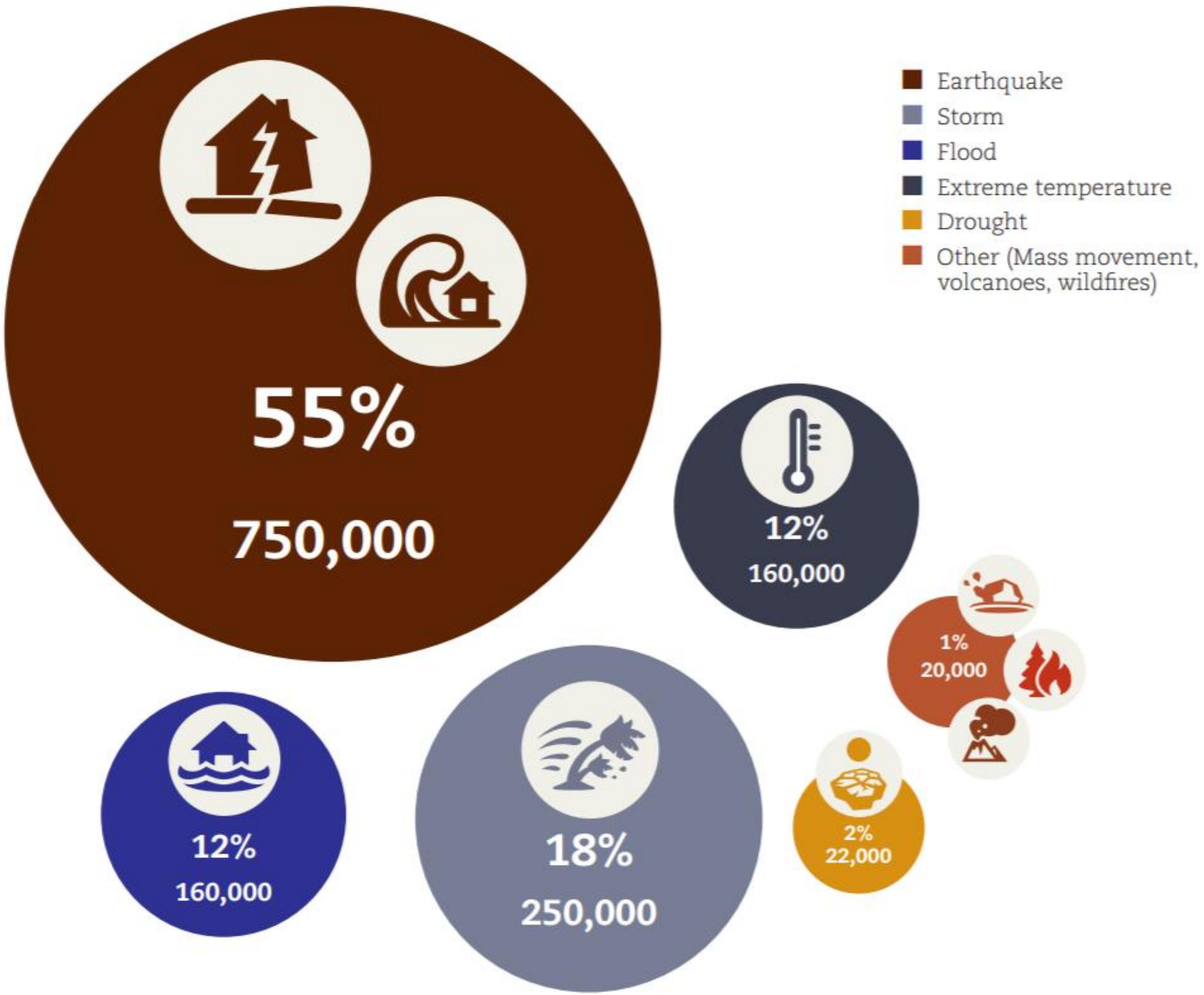

- Floods were the most frequent type of disaster in 1994-2013, accounting for 43% of all events.

- They also affected more people than all other types of natural disaster put together, i.e. 55% of the global total in the past 20 years.

- Floods also became increasing frequent, rising from 123 per year on average between 1994 and 2003 to an annual average of 171 in the period 2004-2013.

Global Runoff Data Center

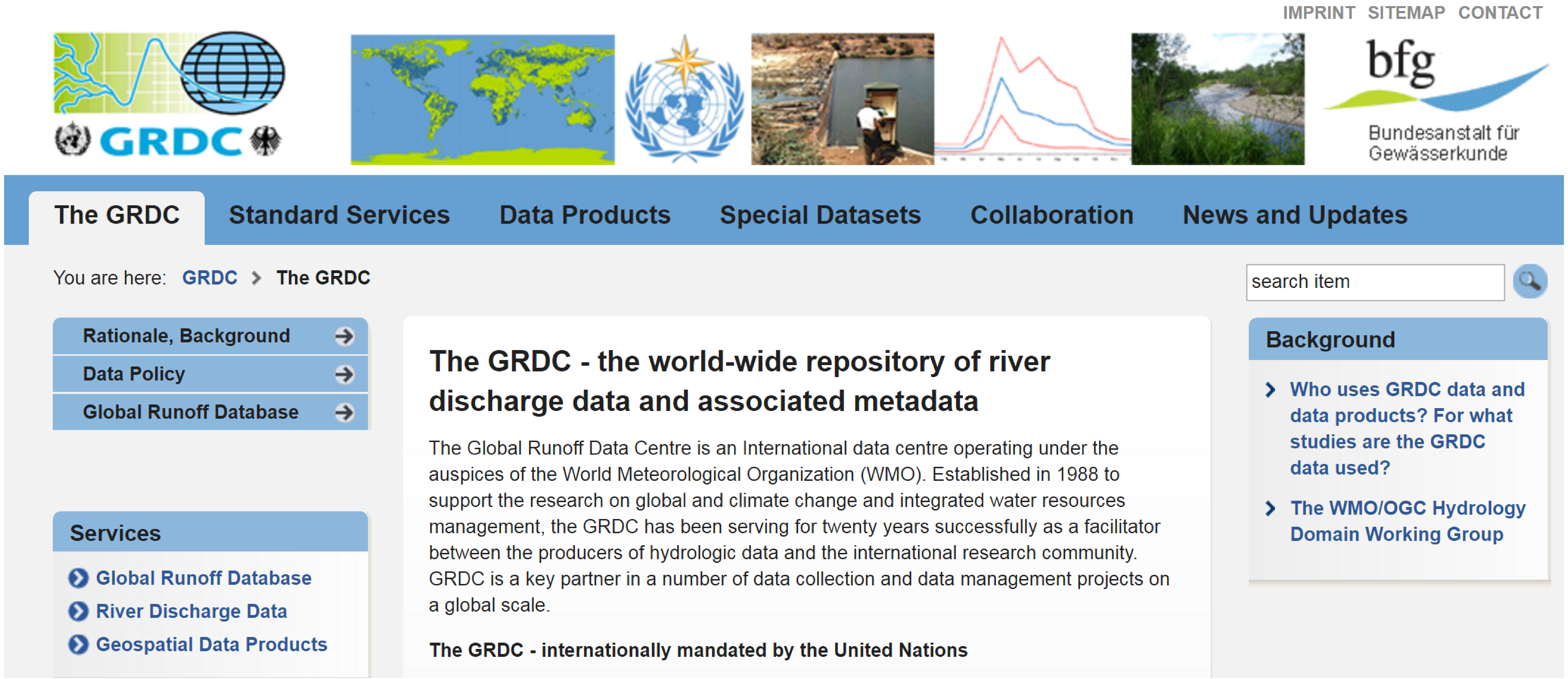

Global Runoff Data Center

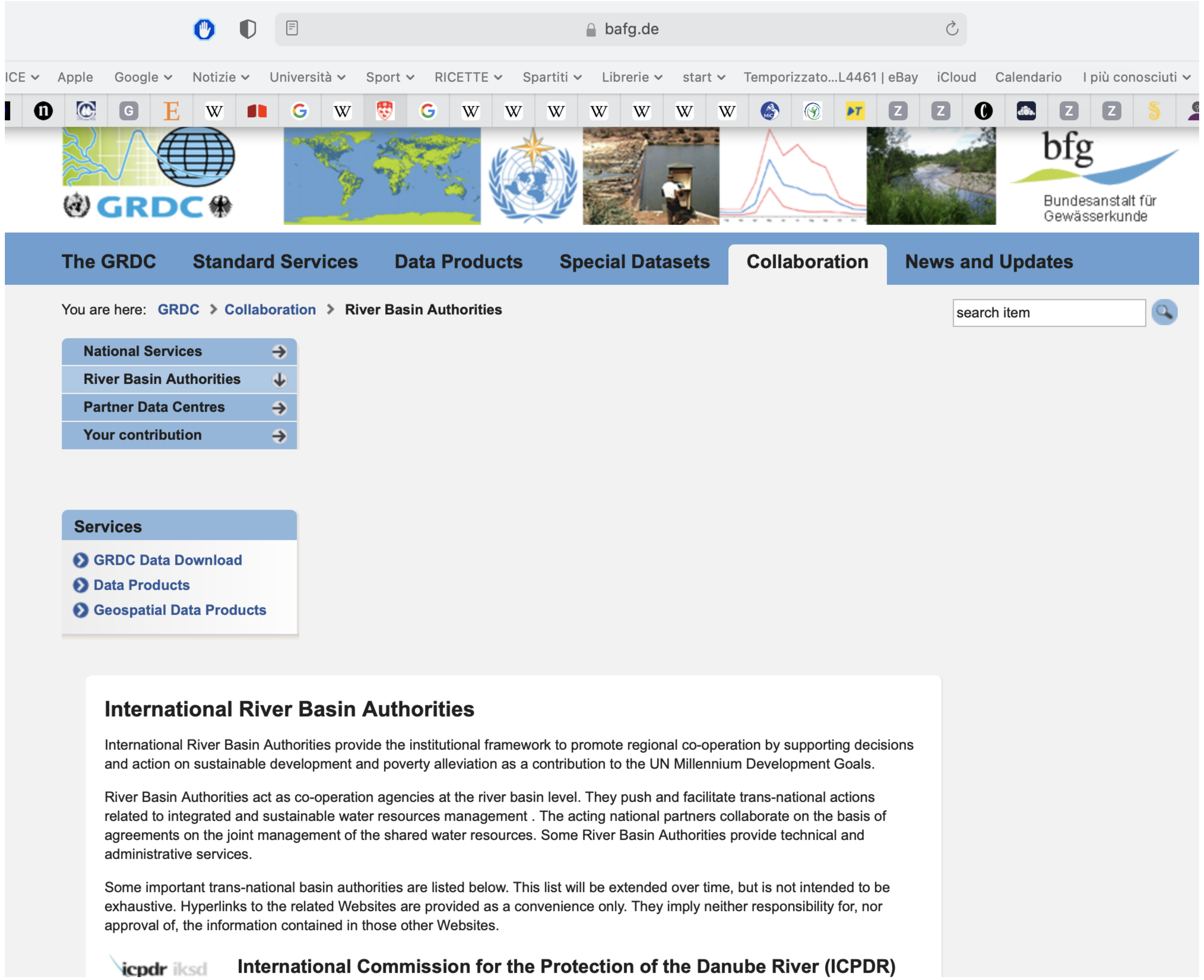

Novità 2020

Volume 1 - Distretto Idrografico Padano

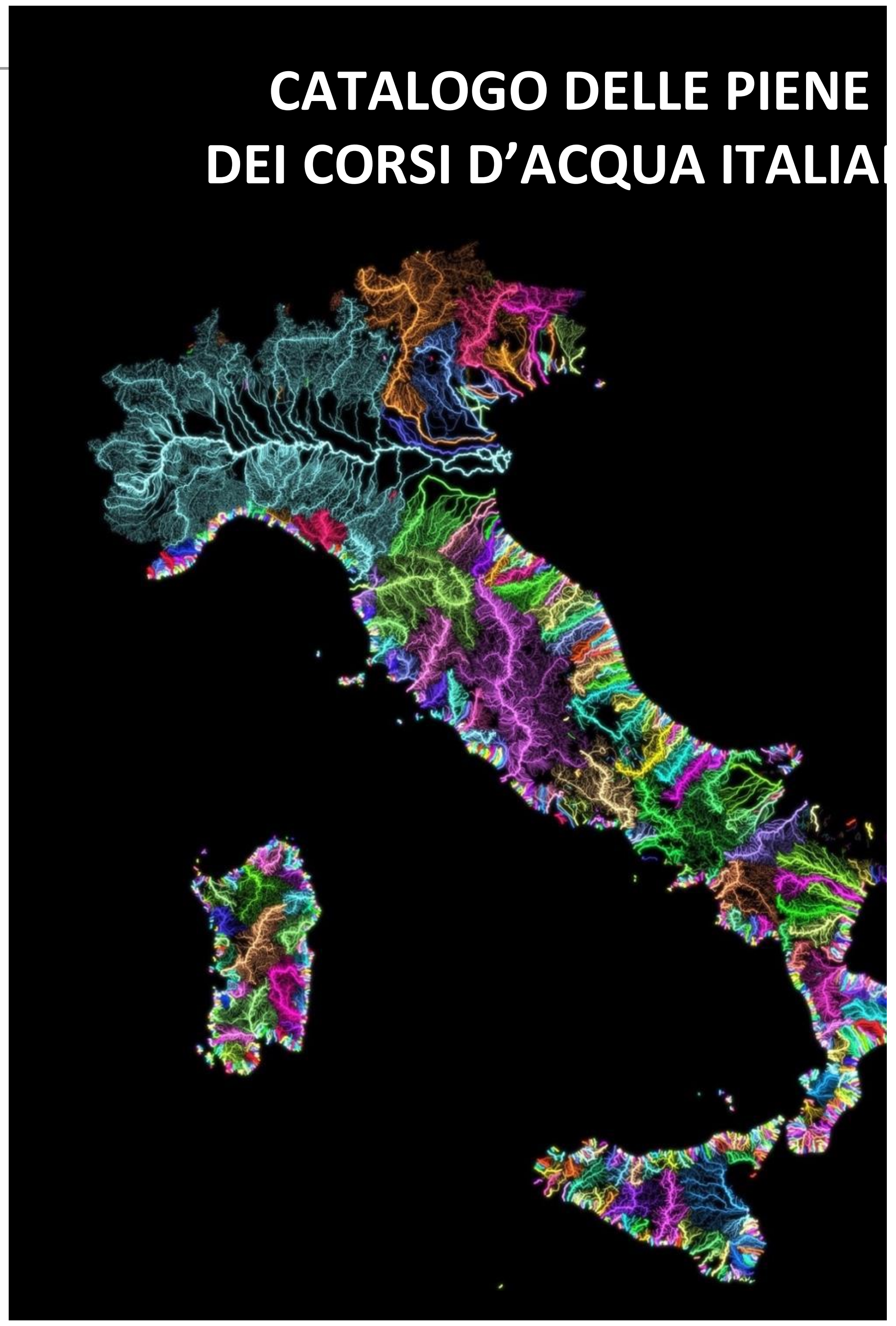

2020

CiNiD
CONSORZIO INTERUNIVERSITARIO PER L'IDROLOGIA

Volume 2 - Distretti Idrografici
Alpi Orientali – Appennino Settentrionale – Appennino Centrale

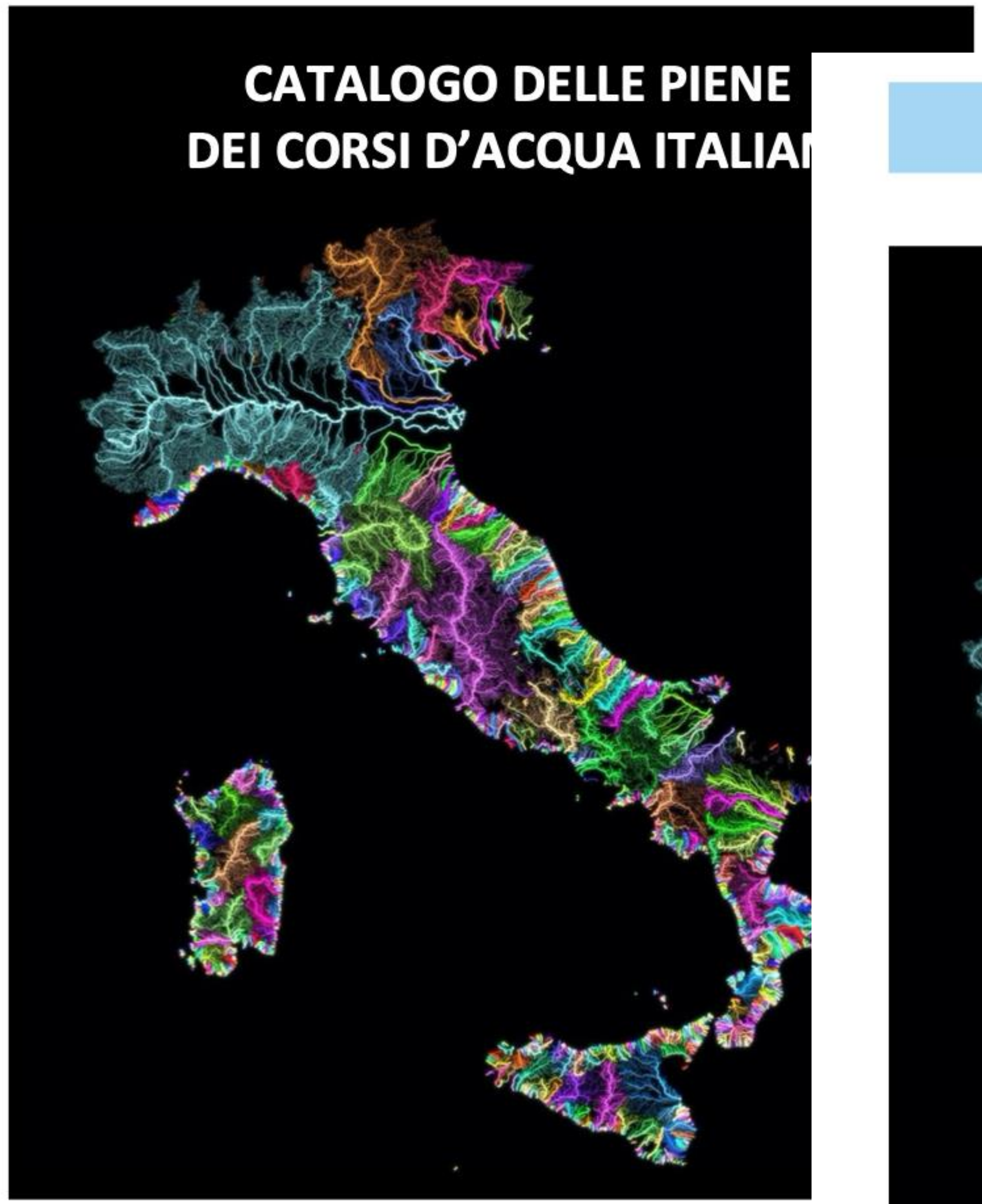

2020

CiNiD
CONSORZIO INTERUNIVERSITARIO PER L'IDROLOGIA

Volume 3 - Distretti Idrografici
Appennino Meridionale – Isole Maggiori

2020

CiNiD
CONSORZIO INTERUNIVERSITARIO PER L'IDROLOGIA

Amazon Kindle store

Global Runoff Data Base

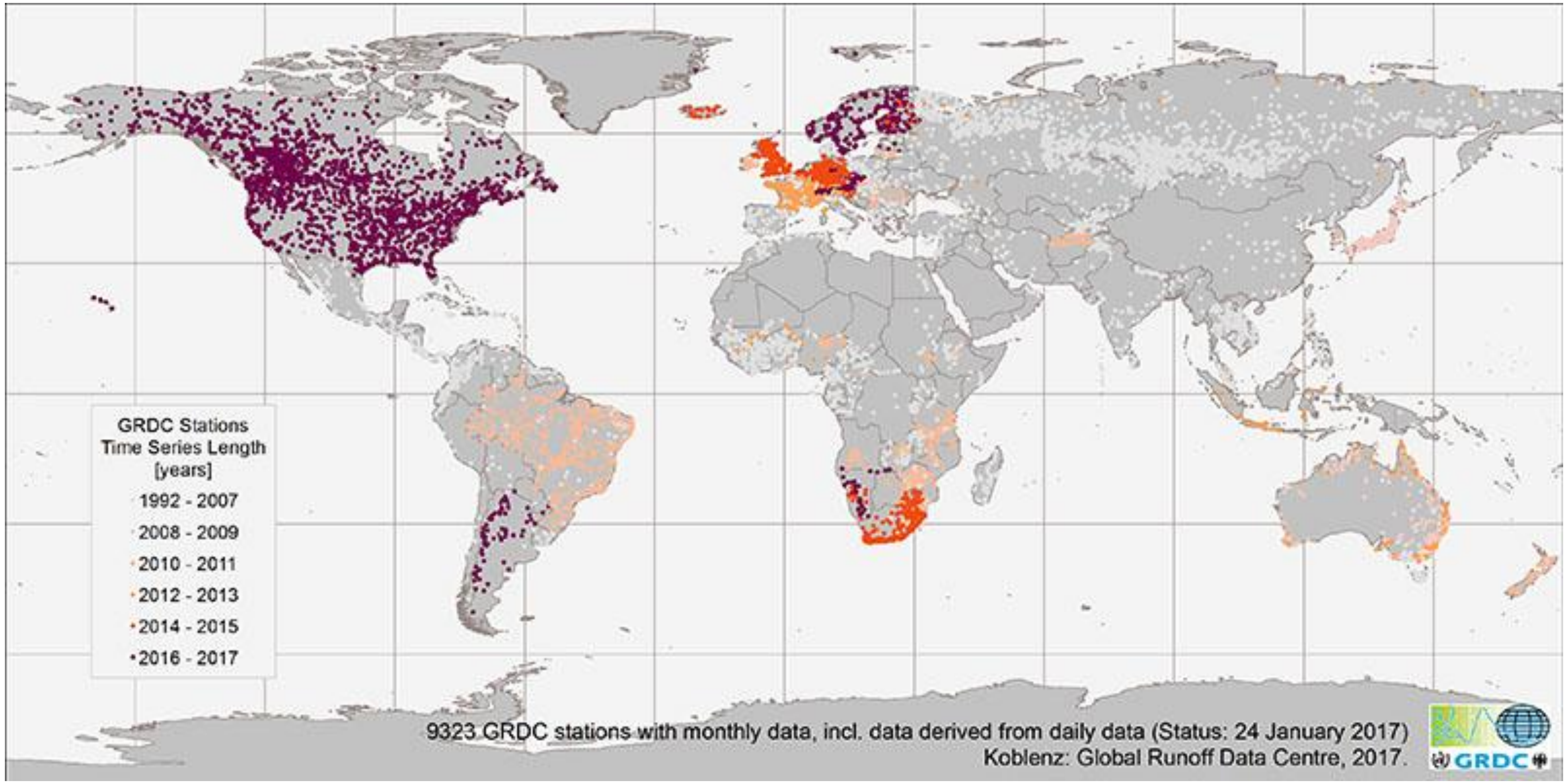

Today the database comprises discharge data of more than 9,300 gauging stations from all over the world.

Accessing and sharing data

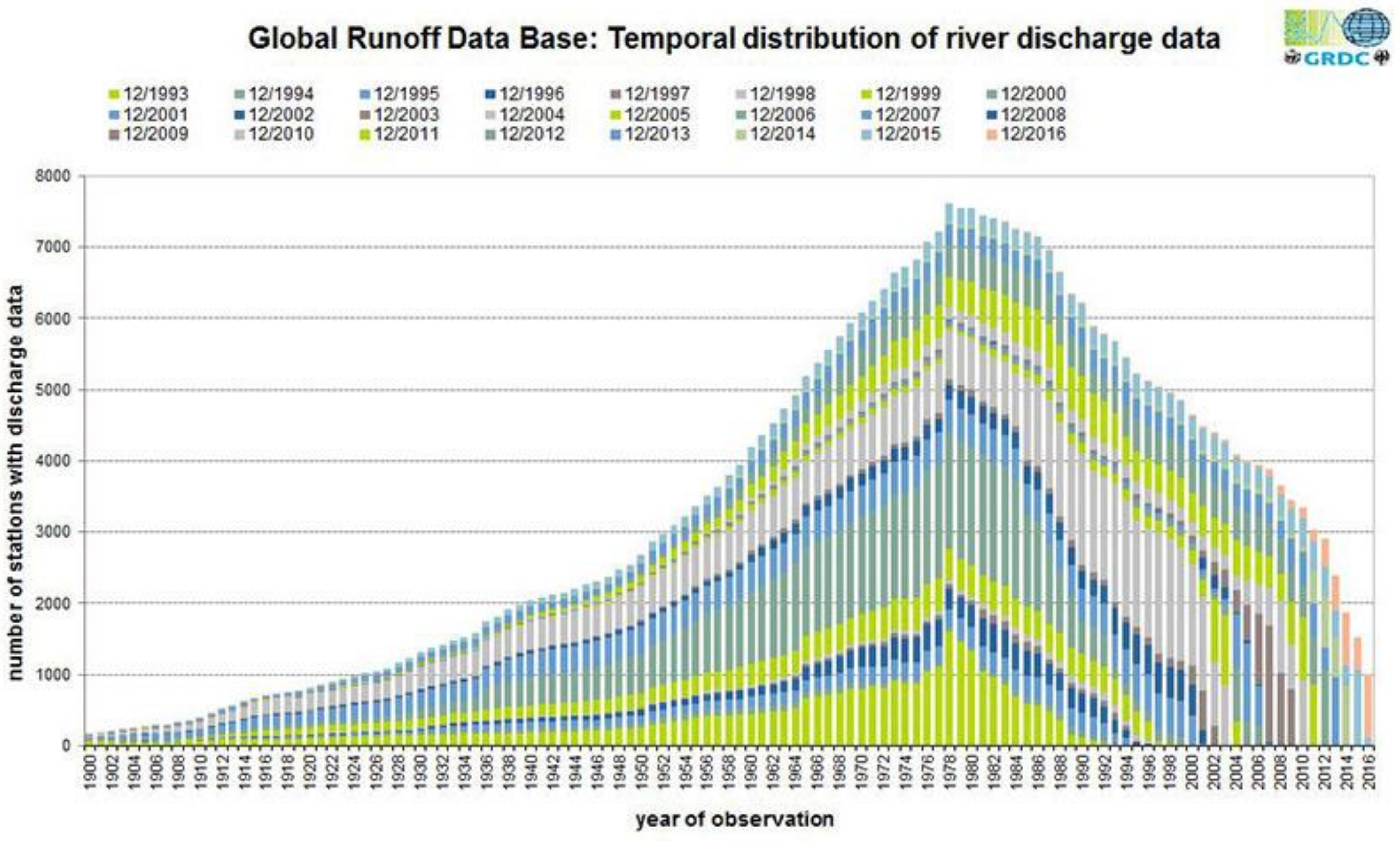

"Given pressures on funding, there is a perceived global threat to the maintenance (never mind expansion) of long-term river flow data archives that cover large geographical domains." (Hannah et al. 2010)

Analysis and Understanding

Panta Rhei
IAHS AISH
Everything Flows

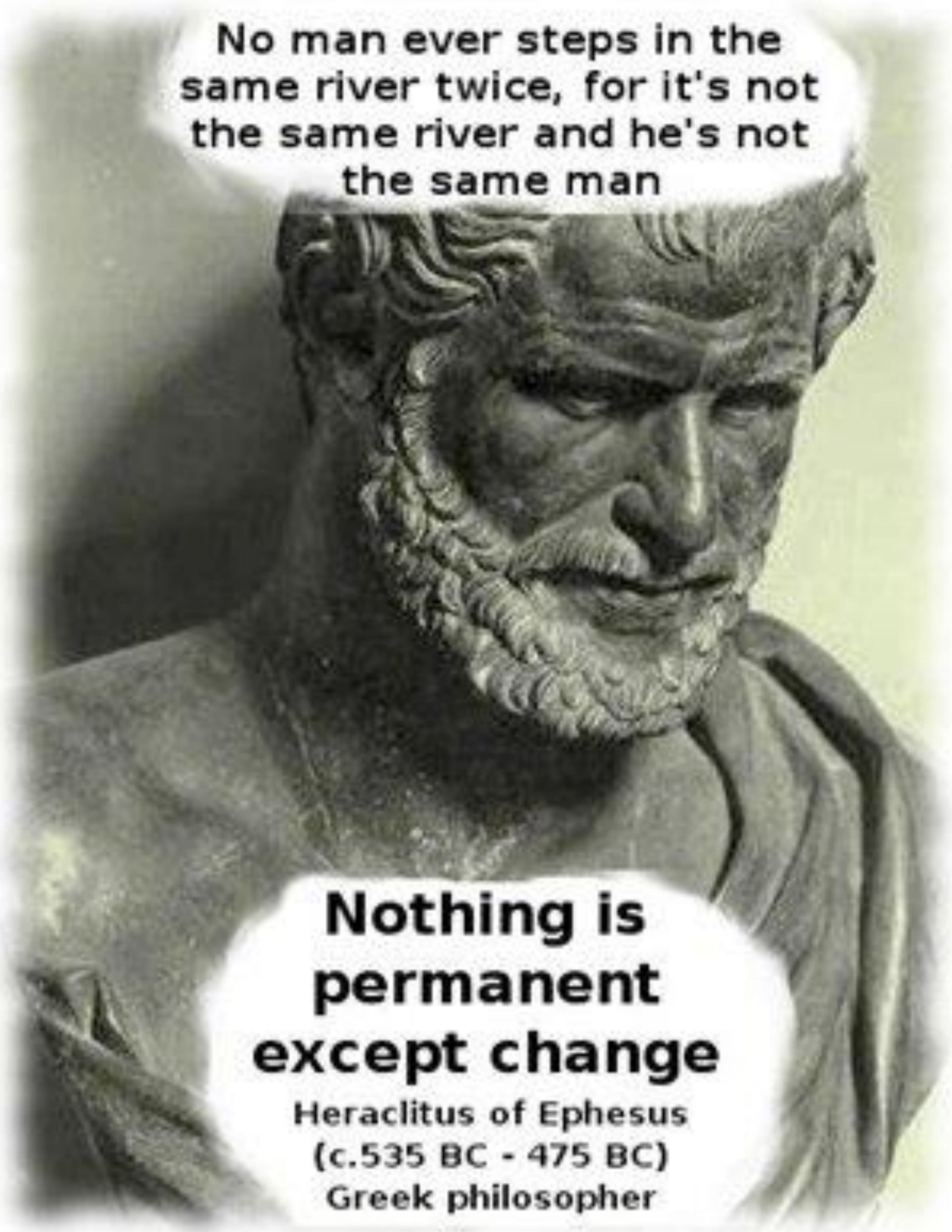

Journal of Hydrology 552 (2017) 28–43

Contents lists available at ScienceDirect

Journal of Hydrology

journal homepage: www.elsevier.com/locate/jhydrol

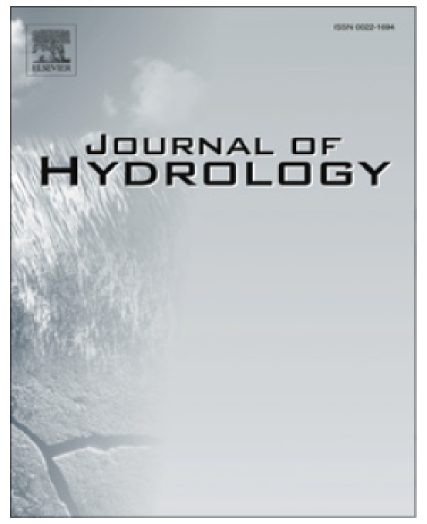

Research papers

A global-scale investigation of trends in annual maximum streamflow

Hong X. Do *, Seth Westra, Michael Leonard

School of Civil, Environmental and Mining Engineering, University of Adelaide, Adelaide, South Australia 5005, Australia

This study investigates the presence of trends in annual maximum daily streamflow data from the Global Runoff Data Centre database.

The records were divided into three reference datasets representing different compromises between spatial coverage and minimum record length, followed by further filtering based on continent, Köppen-Weiger climate classification, presence of dams, forest cover changes and catchment size.

Trends were evaluated using the Mann-Kendall nonparametric trend test at the 10% significance level, combined with a field significance test.

Dataset A2 (3478 stations) comprises stations with at least 30 years annual maximum streamflow over the 1955–2014 period (average record length of 47.6 years).

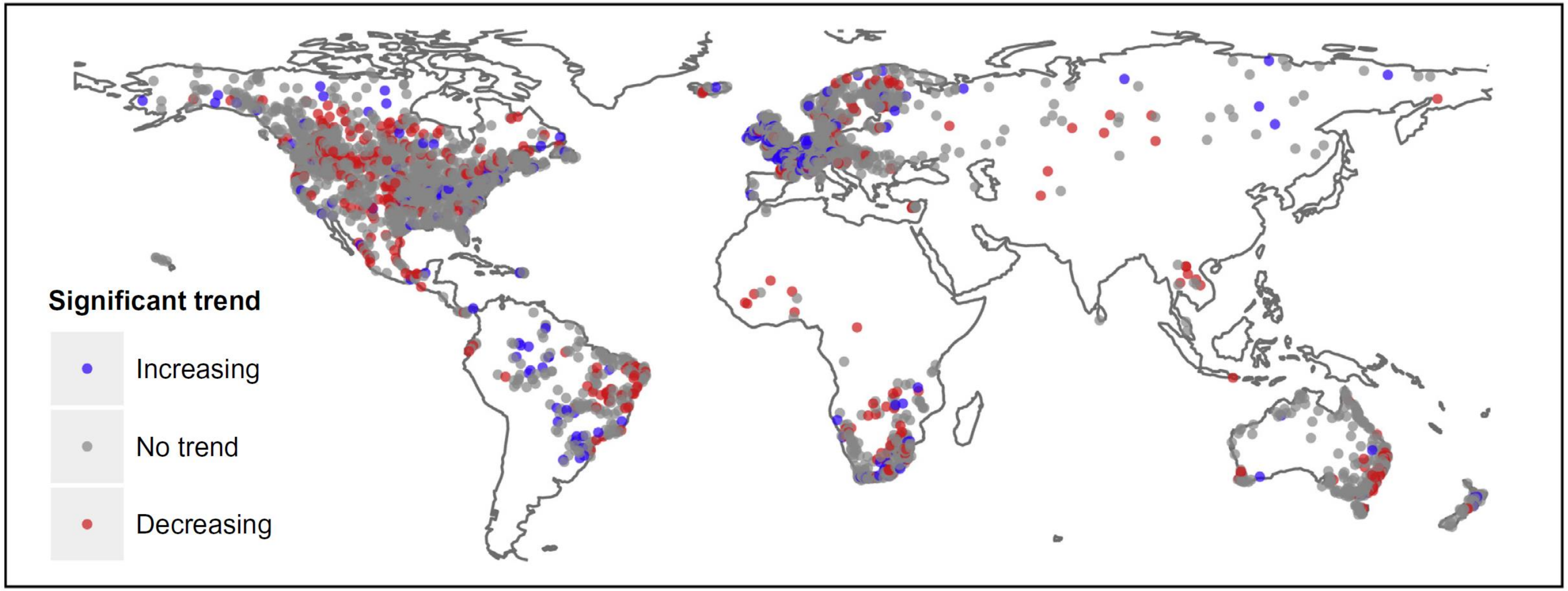

"… over the main reference period (dataset A1; 1966–2005), there were 7.1% of stations with statistically significant increasing trends, and 11.9% of stations with statistically significant decreasing trends. The percentage of stations exhibiting statistically significant increasing trends is consistent with the null hypothesis of no change on average across the global dataset, whereas the percentage of stations showing significant decreasing trends is inconsistent with the null hypothesis"

CLIMATE CHANGE

Stationarity Is Dead: Whither Water Management?

Climate change undermines a basic assumption that historically has facilitated management of water supplies, demands, and risks.

P. C. D. Milly,[1*] Julio Betancourt,[2] Malin Falkenmark,[3] Robert M. Hirsch,[4] Zbigniew W. Kundzewicz,[5] Dennis P. Lettenmaier,[6] Ronald J. Stouffer[7]

"Stationarity is dead because substantial anthropogenic change of Earth's climate is altering the means and extremes of precipitation, evapotranspiration, and rates of discharge of rivers […]. Warming augments atmospheric humidity and water transport. This increases precipitation, and possibly flood risk, where prevailing atmospheric water-vapor fluxes converge."

www.sciencemag.org SCIENCE VOL 319 1 FEBRUARY 2008

Published by AAAS

AGU PUBLICATIONS

Water Resources Research

COMMENTARY

10.1002/2014WR016092

Modeling and mitigating natural hazards: Stationarity is immortal!

Alberto Montanari[1] and Demetris Koutsoyiannis[2]

Taylor & Francis
Taylor & Francis Group

Hydrological Sciences Journal

ISSN: 0262-6667 (Print) 2150-3435 (Online) Journal homepage: http://www.tandfonline.com/loi/thsj20

Negligent killing of scientific concepts: the stationarity case

Demetris Koutsoyiannis & Alberto Montanari

Hydrological Sciences Journal – Journal des Sciences Hydrologiques, 60 (7–8) 2015

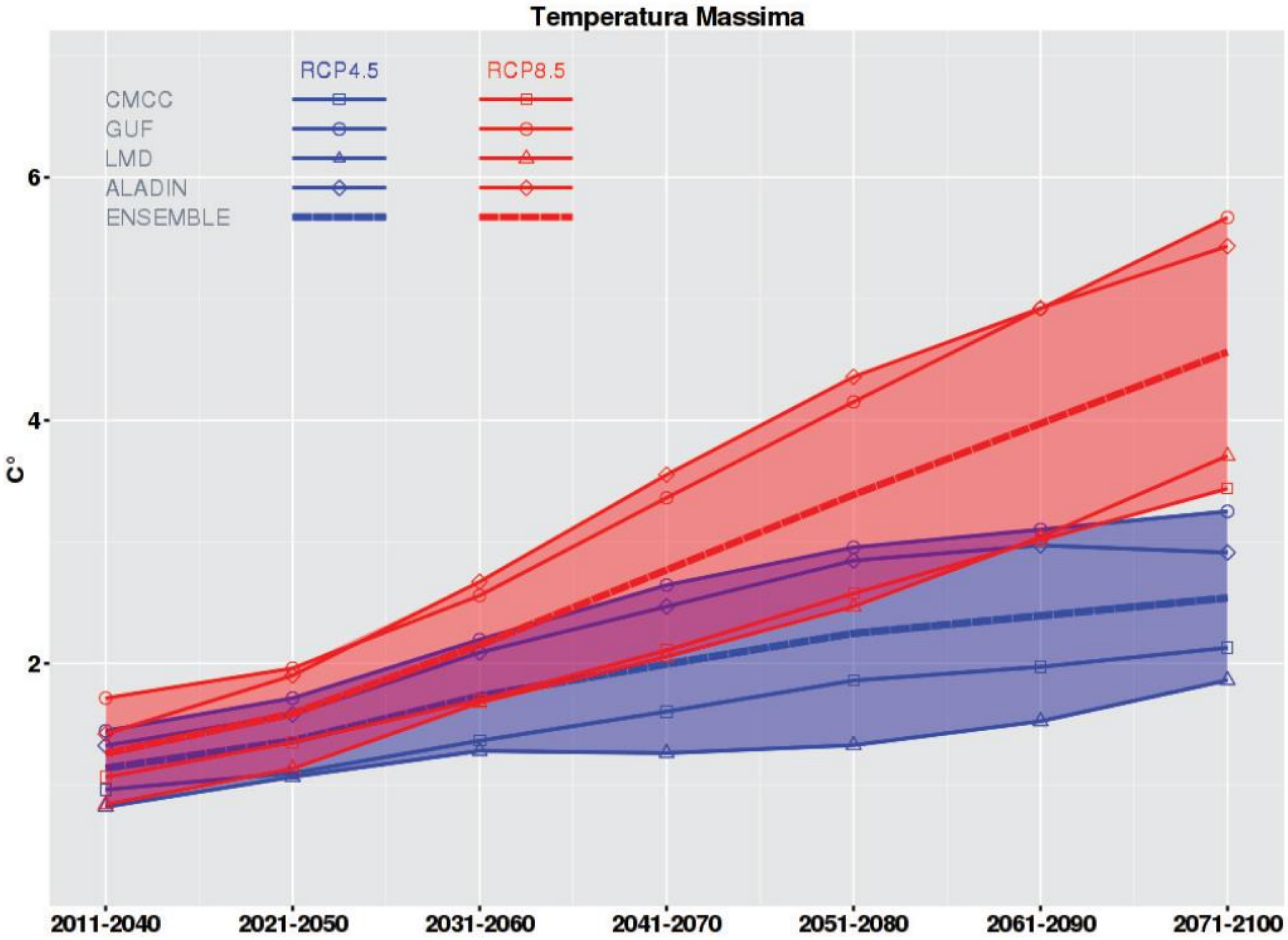

Figura 3.1 – *Temperatura massima. Variazioni rispetto alla media 1971-2000 dei valori previsti dai quattro modelli (media su periodi di 30 anni) nei due scenari RCP4.5 (blu) e RCP8.5 (rosso). L'area colorata rappresenta lo spread delle previsioni dei modelli mentre la linea tratteggiata indica la media delle variazioni previste dai modelli (ensemble mean).*

IPCC - Representative Concentration Pathways – RCP - scenario intermedio

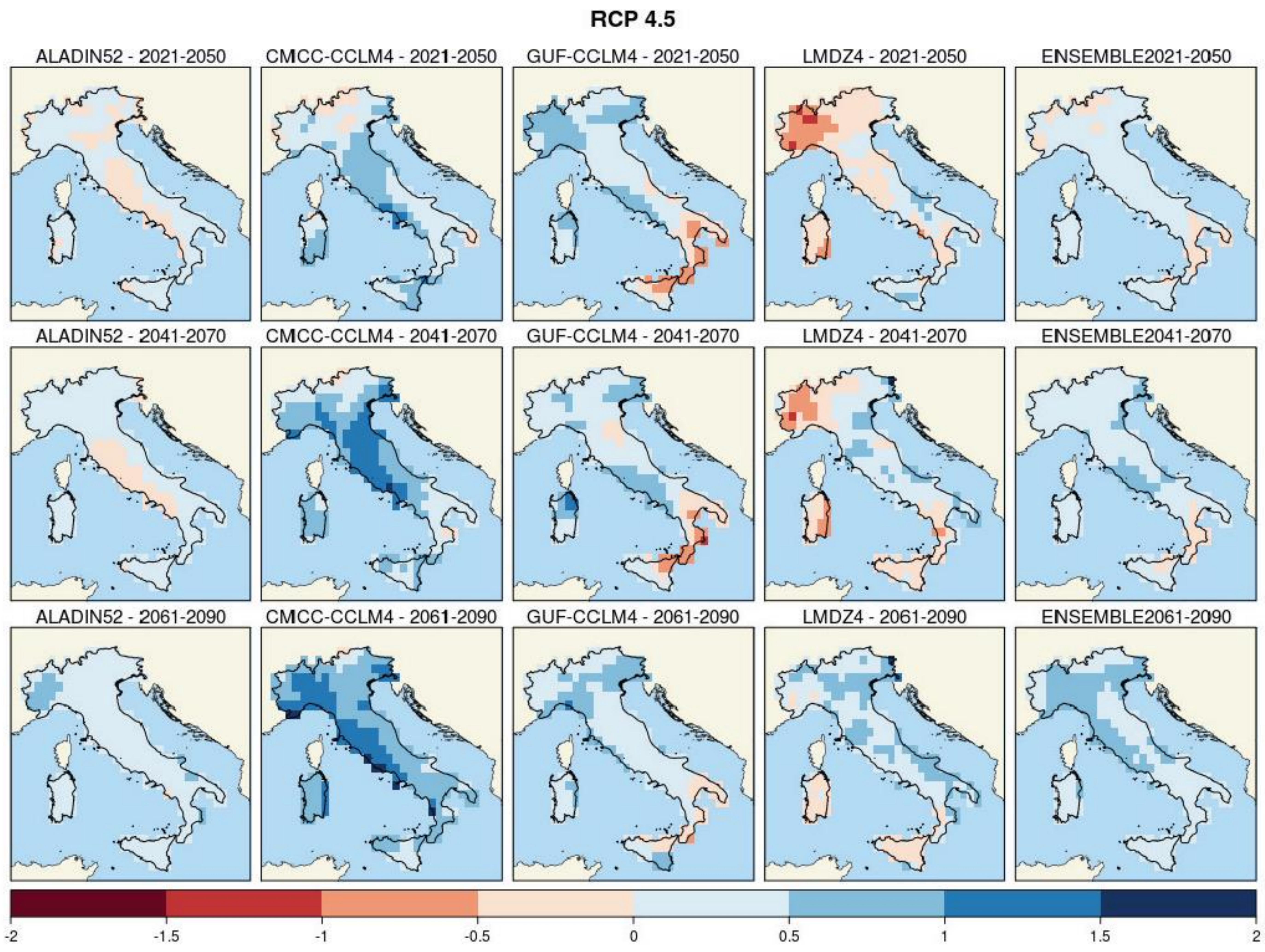

Figura 4.6 – *Intensità di precipitazione giornaliera (mm/giorno), scenario RCP4.5. Mappe delle variazioni previste dai modelli e dall'ensemble mean ai tre orizzonti temporali 2021-2050 (prima riga), 2041-2070 (seconda riga), 2061-2090 (terza riga).*

Revisiting the Concepts of Return Period and Risk for Nonstationary Hydrologic Extreme Events

Jose D. Salas, M.ASCE[1]; and Jayantha Obeysekera, M.ASCE[2]

the concepts of return period and risk are formulated by extending the geometric distribution to allow for changing exceeding probabilities over time

JOURNAL OF HYDROLOGIC ENGINEERING © ASCE / MARCH 2014

Contesto

- The reduction of uncertainty in the estimation of the return period of floods is still one of the main challenges for hydrologists and one of the major needs for flood control agencies;
- Available methodologies are usually limited by the use of extrapolation procedures needed to extend the probability distribution to high return periods.
- The problem becomes particularly complex as less reasonable is felt to be the basic assumption of climatic stationarity, which has driven the scientific research between the 70’s and 90’s.

Contesto

- Althought one may acknowledge that today the best perfoming methods in terms of accuracy of prediction of extremes are still those based on statistic, regional analyses,
- These methods are also generally based on the hypotheses of process stationarity and statistical homogeneity of climatic and physiographic variables.
- Such models are susceptible of improvements and reduction of uncertainty through a deeper analysis of the spatial variability of the hydrological information.

Contesto

- Most procedures for estimating the mean annual flood are still empirical and they are often different from one region to another
- Sometimes statistical regional analysis leads to consider regions different for geology, morphology, climate, etc. as homogeneous

XXXIII Convegno Nazionale di Idraulica e Costruzioni Idrauliche
Brescia, 10-15 settembre 2012

DOPO IL VAPI: LA VALUTAZIONE DELLE MASSIME PORTATE AL COLMO DI PIENA NELL'ESPERIENZA DEL POR CALABRIA

D. Biondi[(1)], P. Claps[(2)], F. Cruscomagno[(1)], D.L. De Luca[(1)], M. Fiorentino[(3)], D. Ganora[(2)], A. Gioia[(4)], V. Iacobellis[(4)], F. Laio[(2)], S. Manfreda[(3)], P. Versace[(1)]

Derived Flood Frequency (DFF)

Peter Eagleson, in 1972, derived the probability distribution of the peak streamflow by integrating the joint density function $g(i_e, t_e, A_r)$ of the rainfall intensity i_e, rainfall duration t_e and contributing area to the peak flow A_r :

$$G_Q(q) = prob[Q < q] = \iiint_{R(q)} g(i_e, t_e, A_r) di_e dt_e dA_r$$

- *R(q):* Domain of *ie*, *te* and *Ar*, that provide Q<q.

Iacobellis and Fiorentino (*IF*) model

WRR (2000, 2001):

The variate: Peak of direct stream flow:

$$Q = u_a a$$

u_a = peak runoff from the contributing (source) area

a = contributing area to the peak flow.

The peak flow cumulative distr'n function:

$$G_Q(q) = \int_0^A \int_0^{\frac{q}{a}} g(u \mid a) g(a) \, du \, da$$

g(*u*|*a*) = pdf of u conditional on *a*;

g(a) = pdf of a.

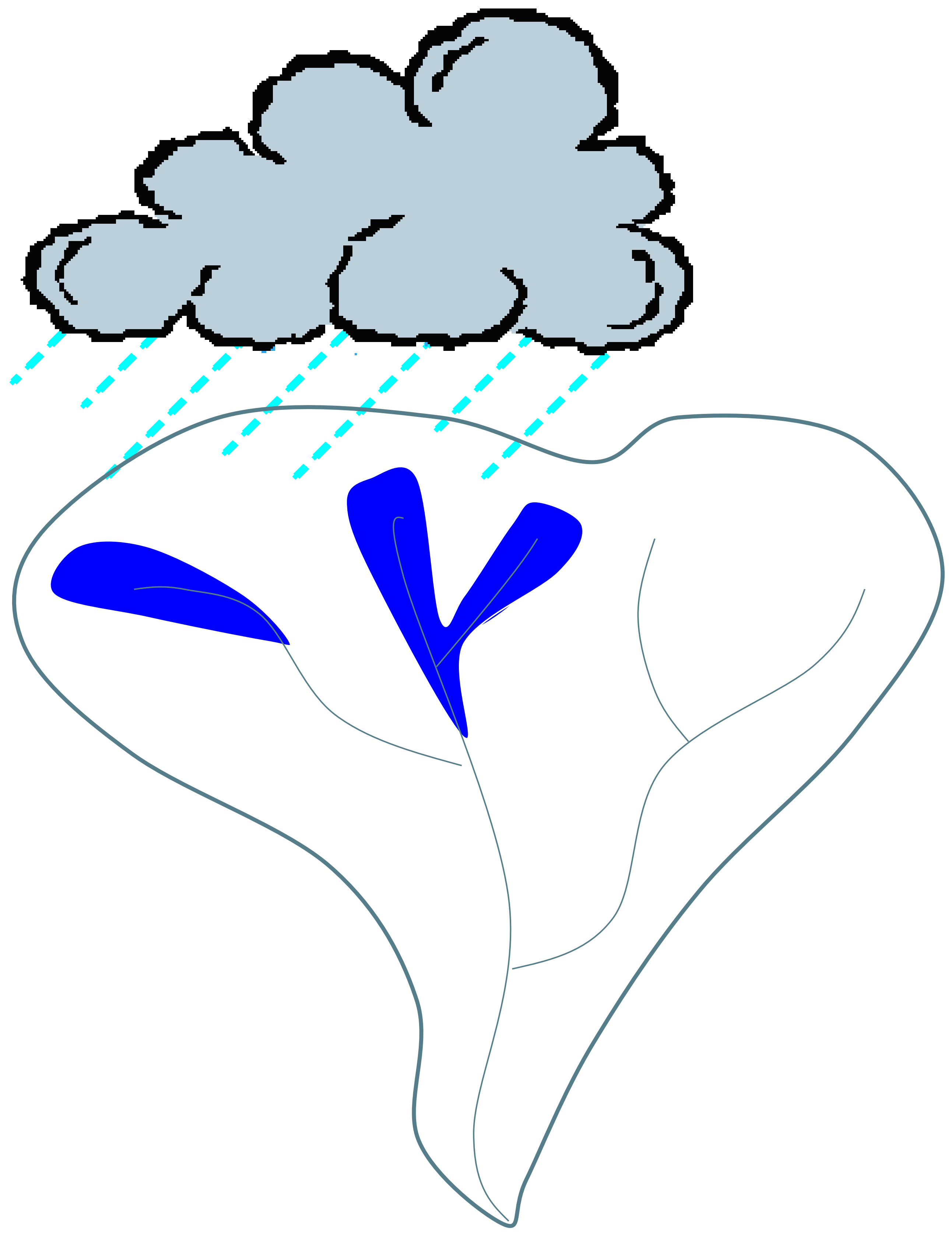

Basin Outlet

IF model:

the contributing area is assumed gamma distributed

$$g(a) = \frac{1}{\alpha\Gamma(\beta)}\left(\frac{a}{\alpha}\right)^{\beta-1}\exp\left(-\frac{a}{\alpha}\right)$$

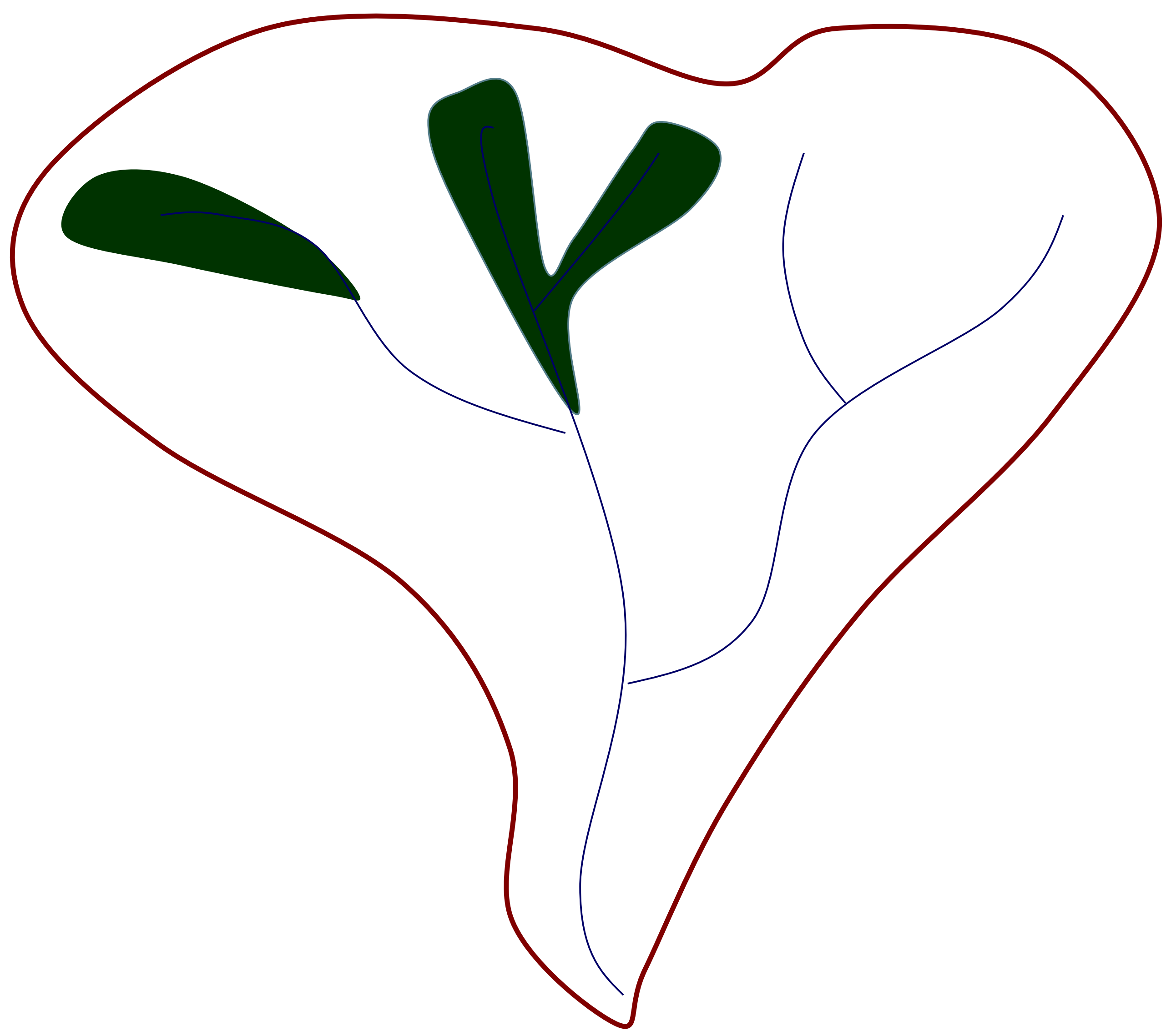

$$\alpha = \frac{E[a]}{\beta} \quad \text{and} \quad r = \frac{E[a]}{A}$$

IF model:

why the contributing area is gamma distributed?

- **this function arises as the distribution of the sum of β stochastic (independent) variables exponentially distributed with equal mean value α.**
- **the flood peak can be thought as the superposition of flows coming from a number of sub-basins which can be differently interested by the storm.**
- **β can be found as the number of sub-basins of Horton order immediately smaller than that of the whole basin. According to a well consolidated geomorphologic knowledge, it tends to be invariant at any scale and assumes values ranging between 3 and 5 in nearly all cases (*Horton*, 1945) with expected value equal to 4.**

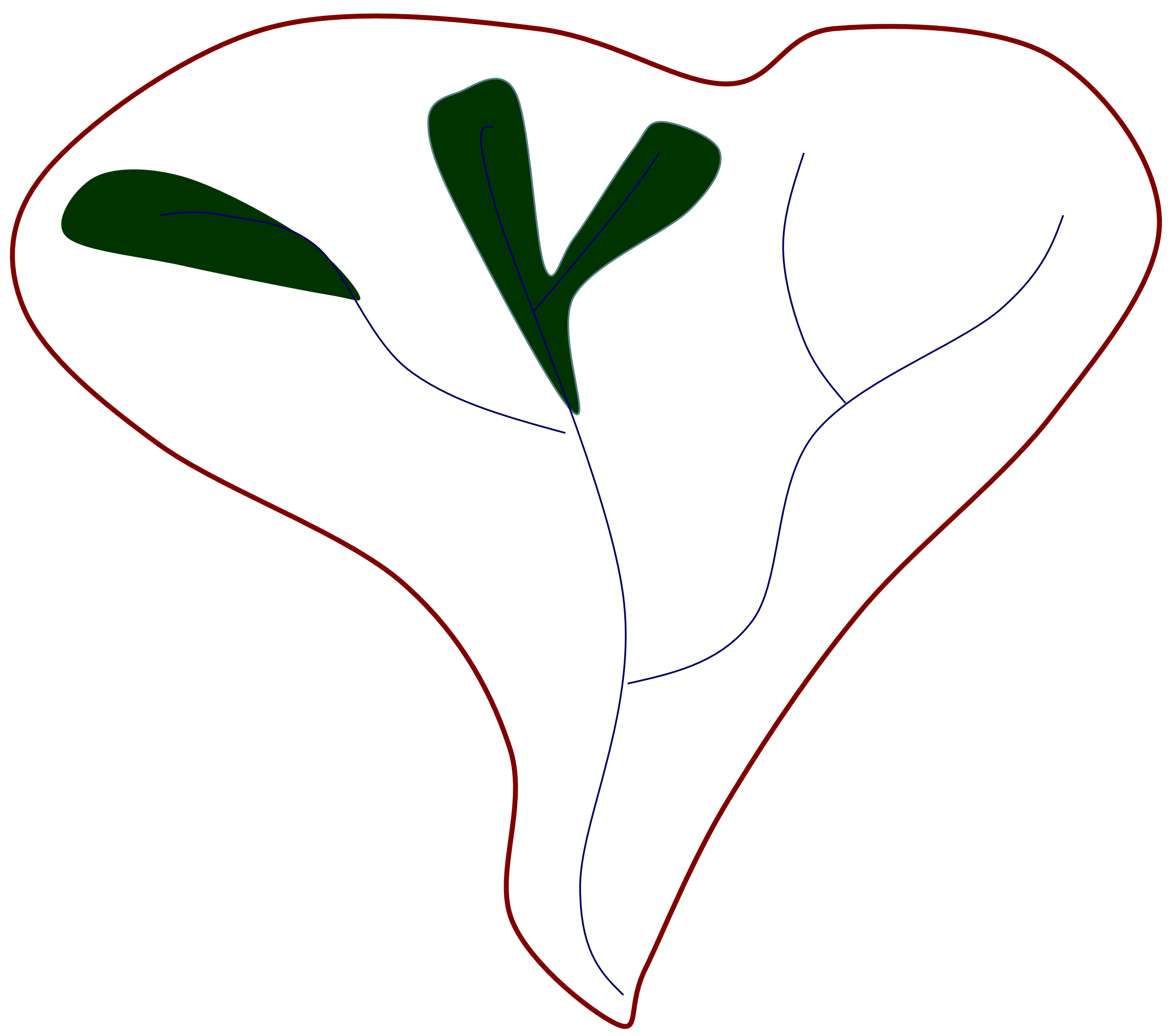

IF model:

Basic hypotheses

The lag-time is assumed to scale with the contributing area by a power law

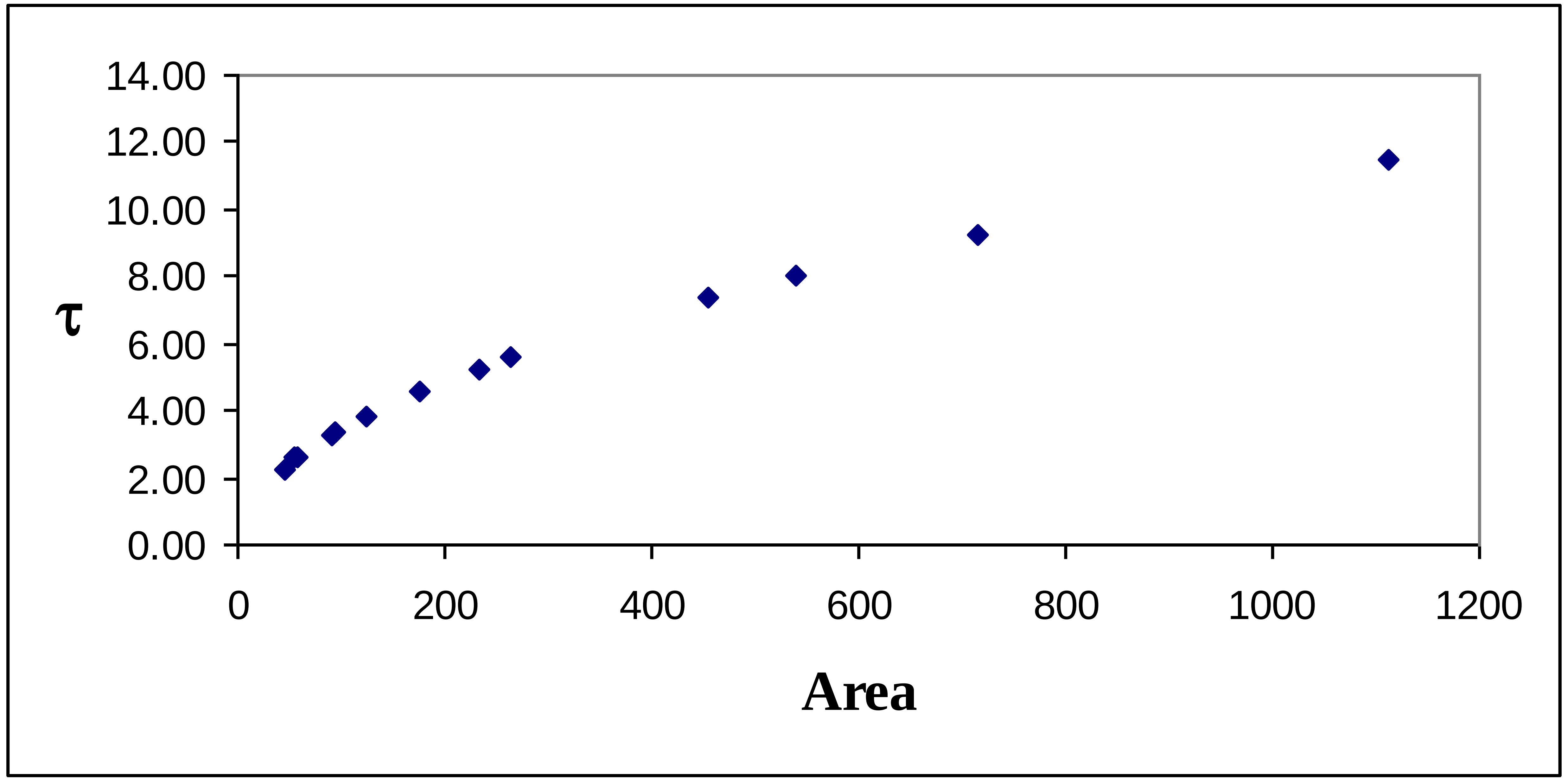

- The flood peak is mainly due to runoff generated in a duration equal to the lag time τ of the contributing area
- Both concentration process and hydrological losses mainly depend on the contributing area

$$u_a = \xi \ (i_{a,\tau} - f_a)$$

The areal rainfall intensity is considered

Weibull distributed

$$g(i_a \mid a) = \frac{k}{E[i_a \mid a]^k} i_a^{\,k-1} \exp\left[-\left(\frac{i_a}{E[i_a \mid a]} \right)^k \right]$$

$$E[i_a \mid a] = E[i_A] \cdot \left(\frac{a}{A} \right)^{-\varepsilon}$$

IF model:

rainfall modeling

p_1 ed *n* are parameters of the intensity duration curve.

$$\mu_I = p_1 \tau_{(rA)}^{\,n-1}$$

$$E[i_A] = \frac{p_1 \tau_A^{n-1}\left[1-\exp\left(-1.1\tau_A^{0.25}\right)+\exp\left(-1.1\tau_A^{0.25}-0.004A\right)\right]}{\Lambda_p S_{\Lambda_p}}$$

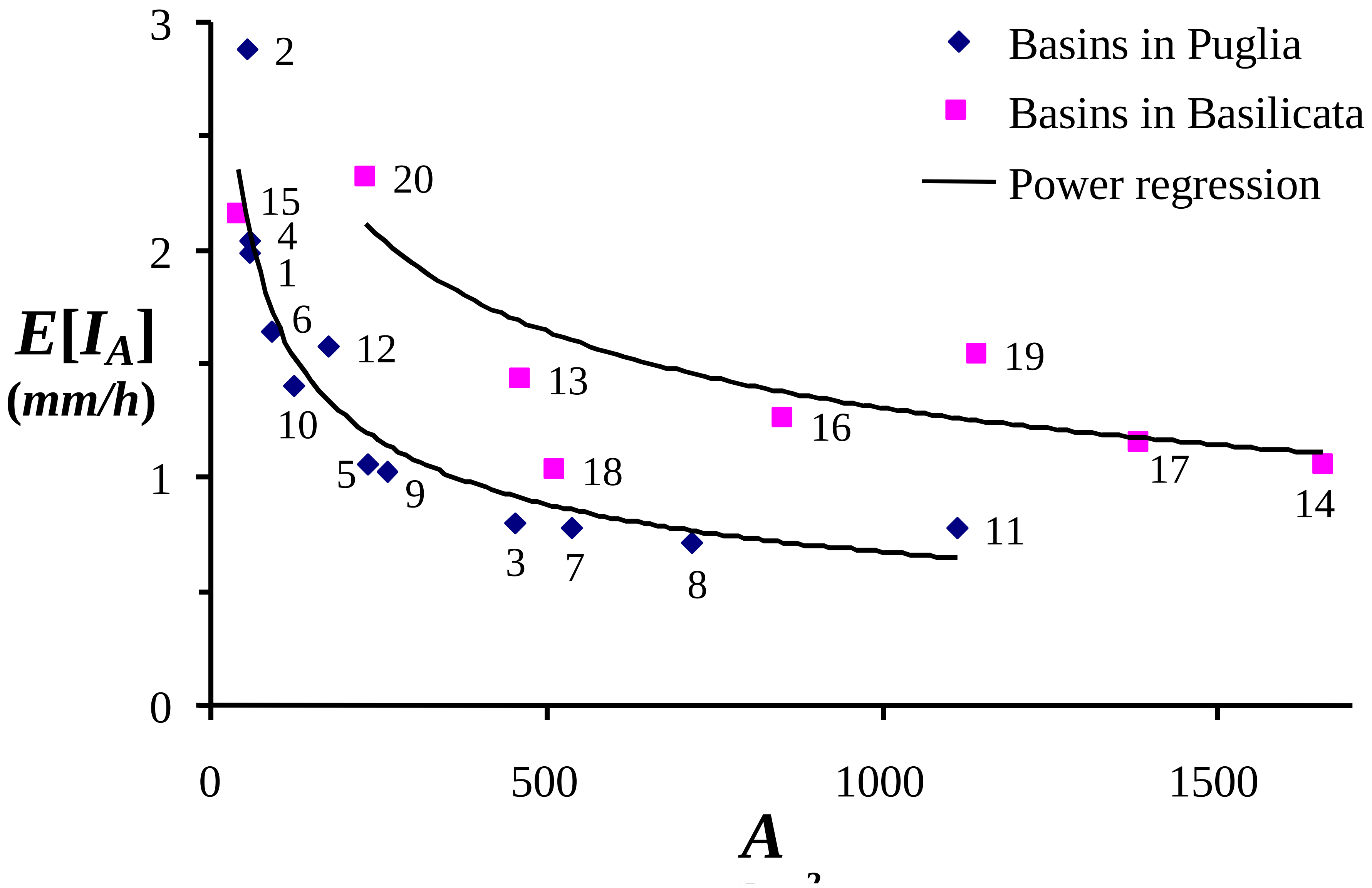

The expected value of the space-time averaged rainfall intensity occurring in a duration *t scales with a according to a power law.*

$$E\,[i_{a,t}] = i_A (a/A)^{-\varepsilon}$$

IF model:

hydrological losses

---

f_a scales with the basin area. $f_a = f_A\,(a/A)^{-\varepsilon'}$

Also, under the assumption of a rainfall process with Poisson occurrences and Weibull distributed intensity, the spatial average water loss f_A is related to the ratio between the average annual rates of rainfall and flood events, respectively Λ_p and Λ_q, as

$$f_A = \frac{E[i_A]}{\Gamma(1+1/k)}\left[\log\left(\frac{\Lambda_p}{\Lambda_q}\right)\right]^{1/k}$$

IF model:

the Derived Distribution

Under the hypothesis of compound Poisson processes of independent floods, the annual maxima flood probability distribution is:

$$F_{Q_p}(q_p) = 1 - \frac{1}{T} = \exp\left[-\Lambda_q\left(1 - G_{Q_p}(q_p)\right)\right]$$

$$F_{Q_p}(q_p) = \exp\left\{-\Lambda_q \int_0^A \left[\left(\frac{1}{\alpha\Gamma(\beta)}\left(\frac{a}{\alpha}\right)^{\beta-1} \exp\left(-\frac{a}{\alpha}\right) + \delta(a-A)P_A\right) \exp\left(-\frac{\left(\left(q_p - q_o\right)/(\xi a) + f_A\,(a/A)^{-\varepsilon'}\right)^k - \left(f_A\,(a/A)^{-\varepsilon'}\right)^k}{\left(i_A\,(a/A)^{-\varepsilon}/\Gamma(1+1/k)\right)^k}\right)\right] da\right\}$$

Model consistency: estimated parameters are in the expected range, pdf's of contributing areas are consistent with prevailing runoff generation mechanisms

Flood peaks CDFs *Contributing areas PDFs*

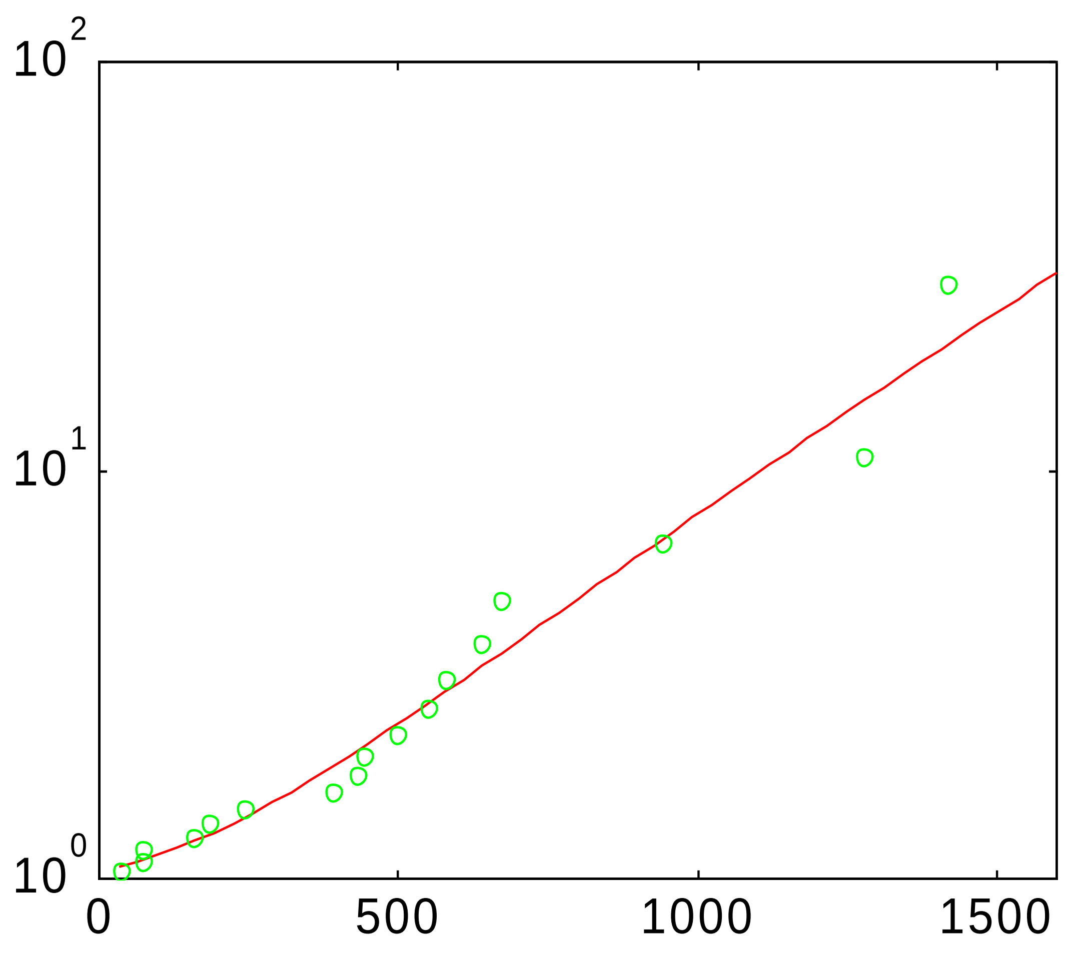

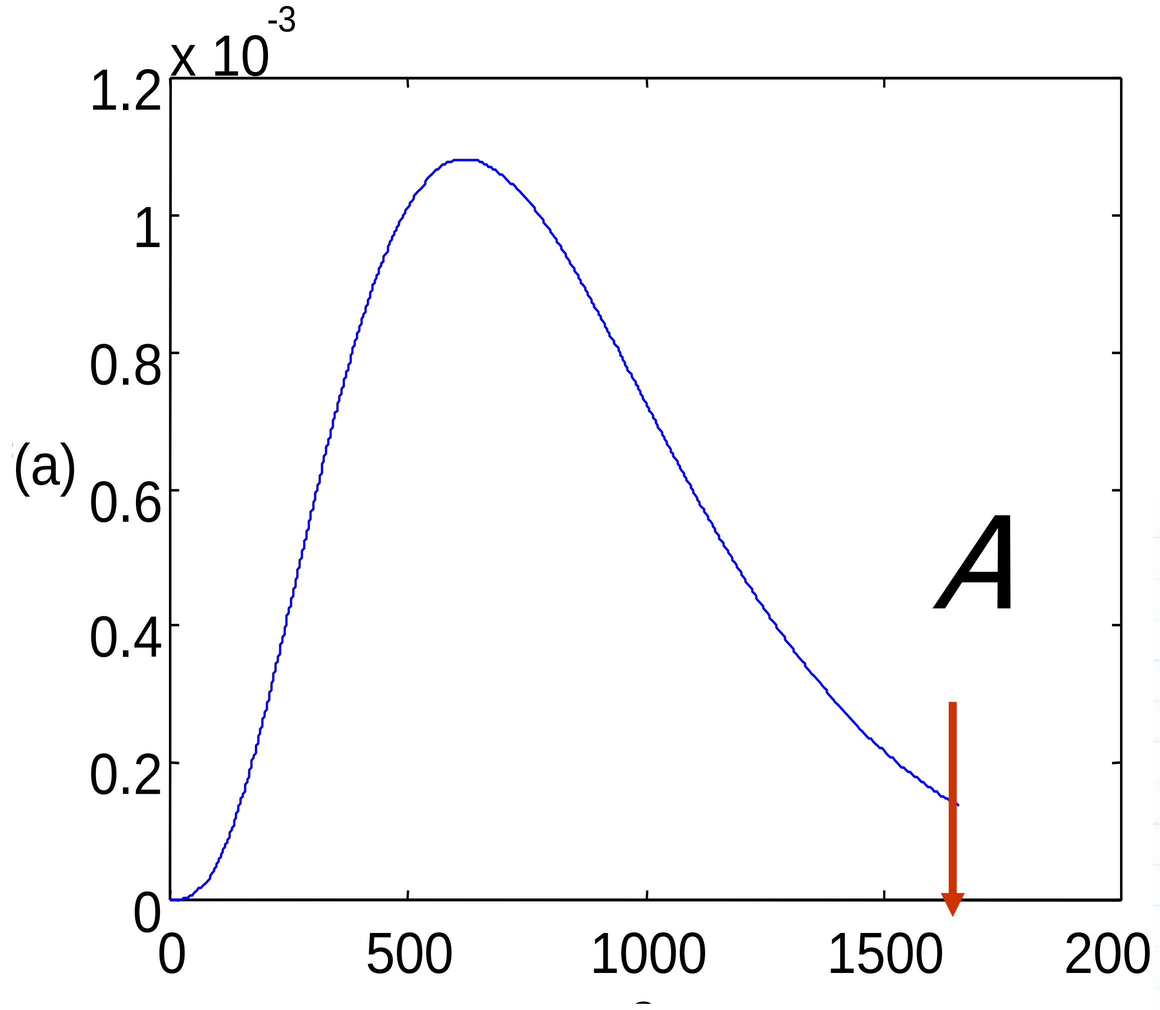

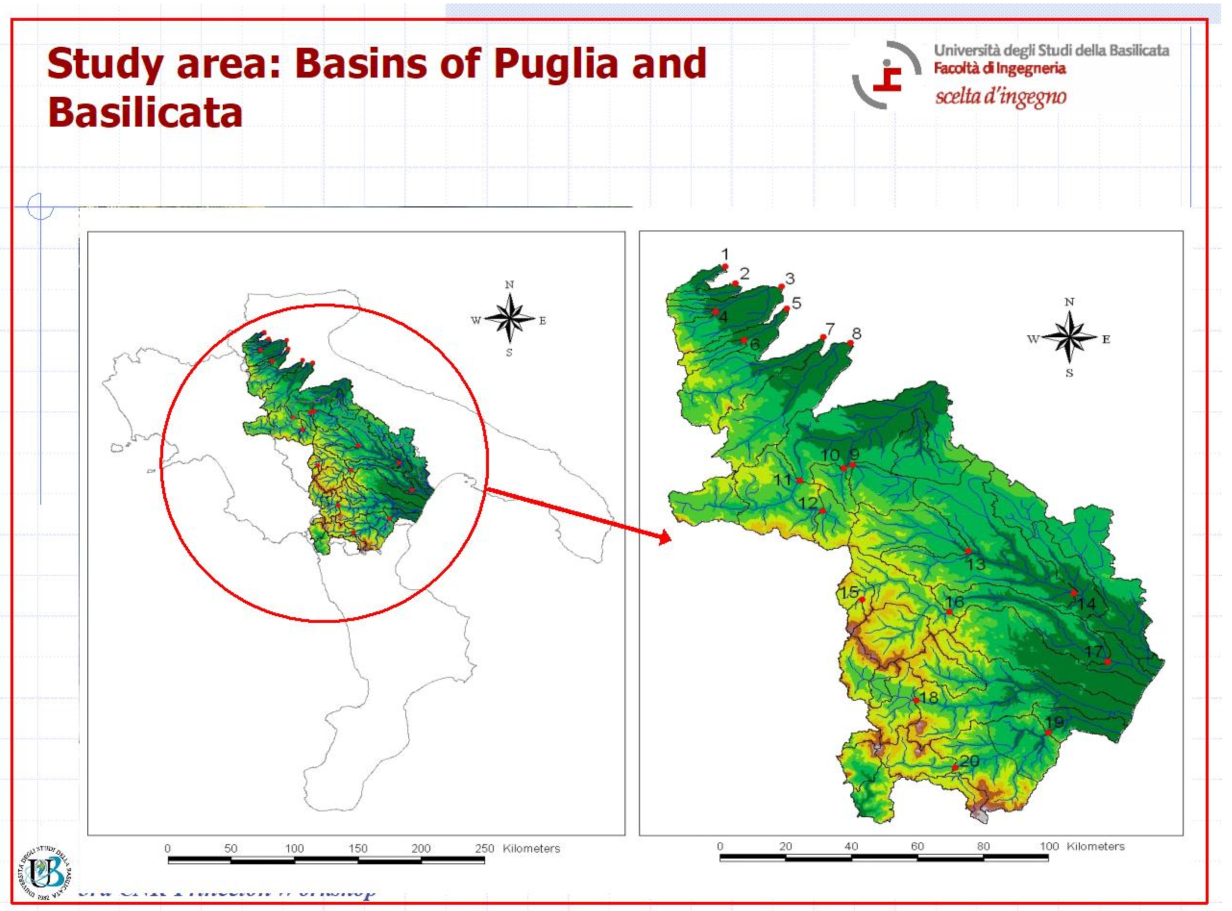

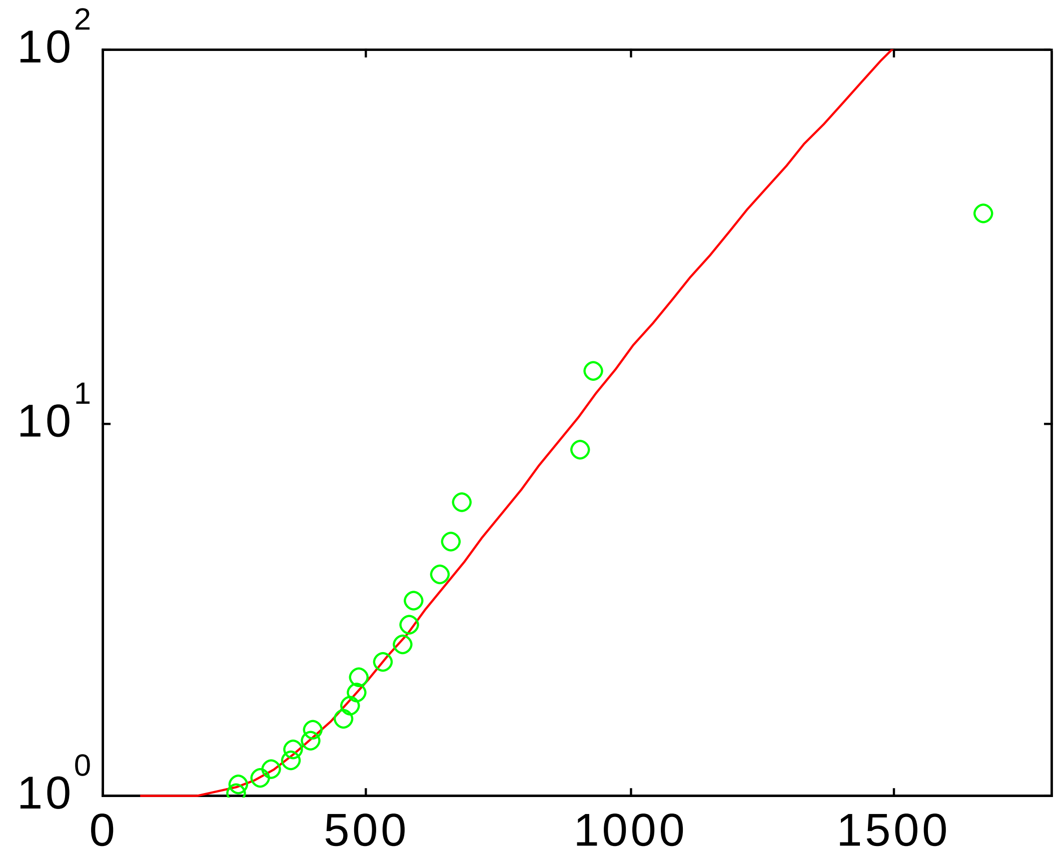

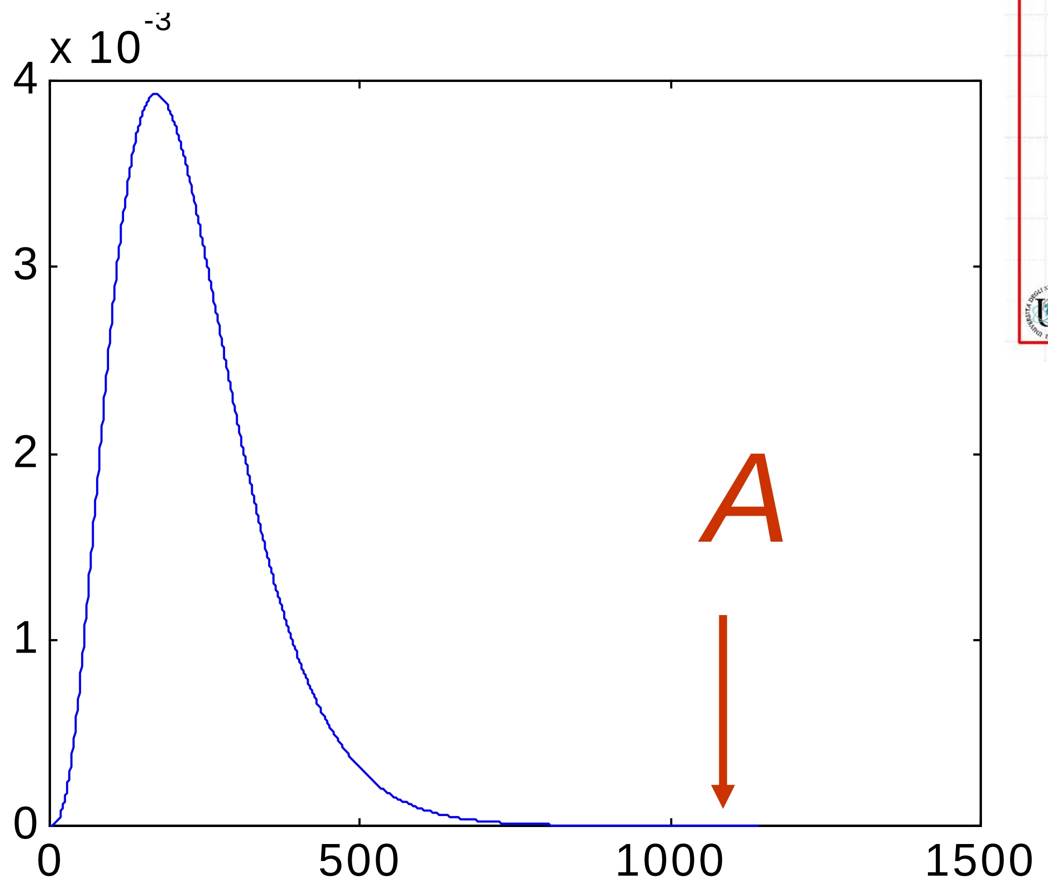

Iacobellis & Fiorentino (2000)

Model consistency: hydrological losses

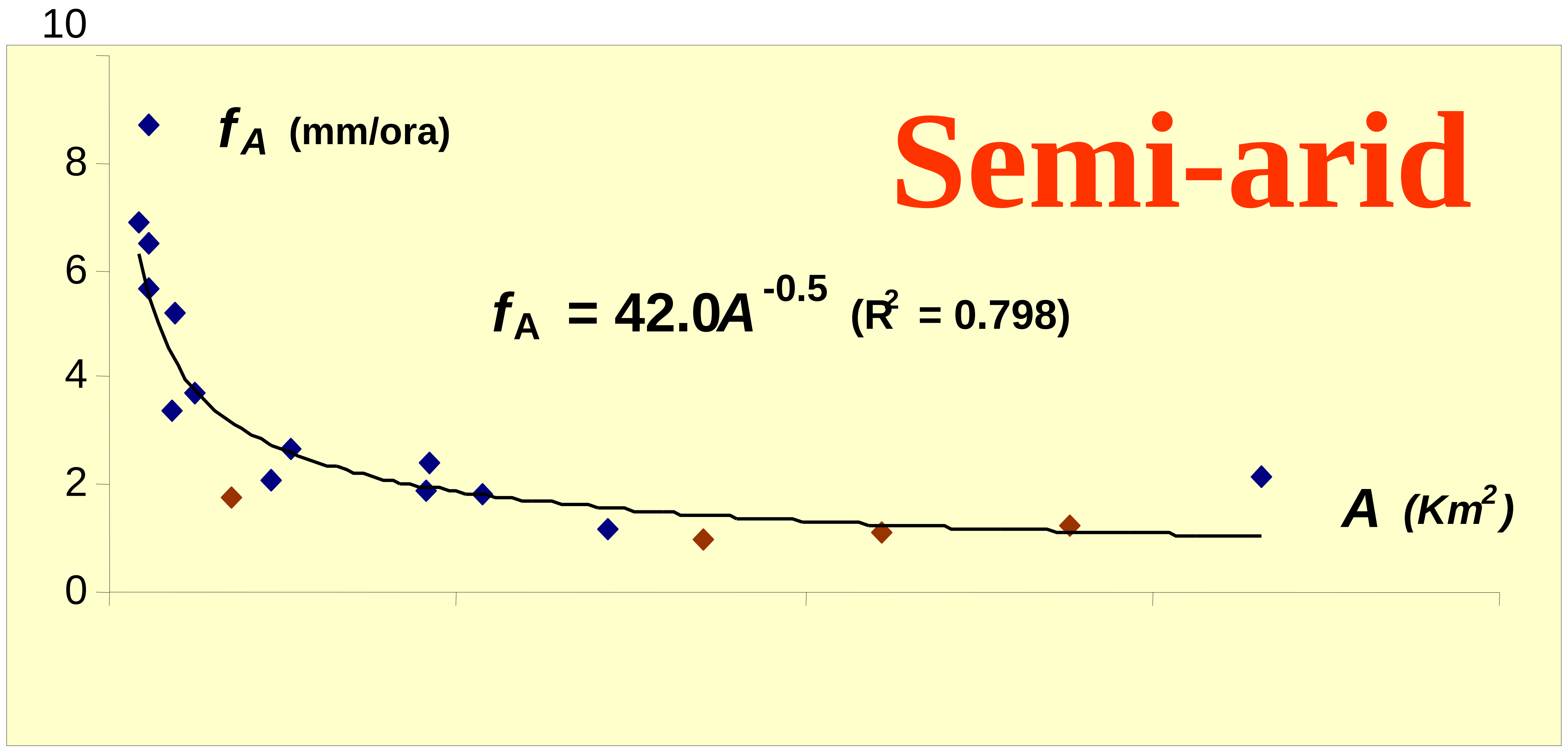

Model consistency: hydrological losses

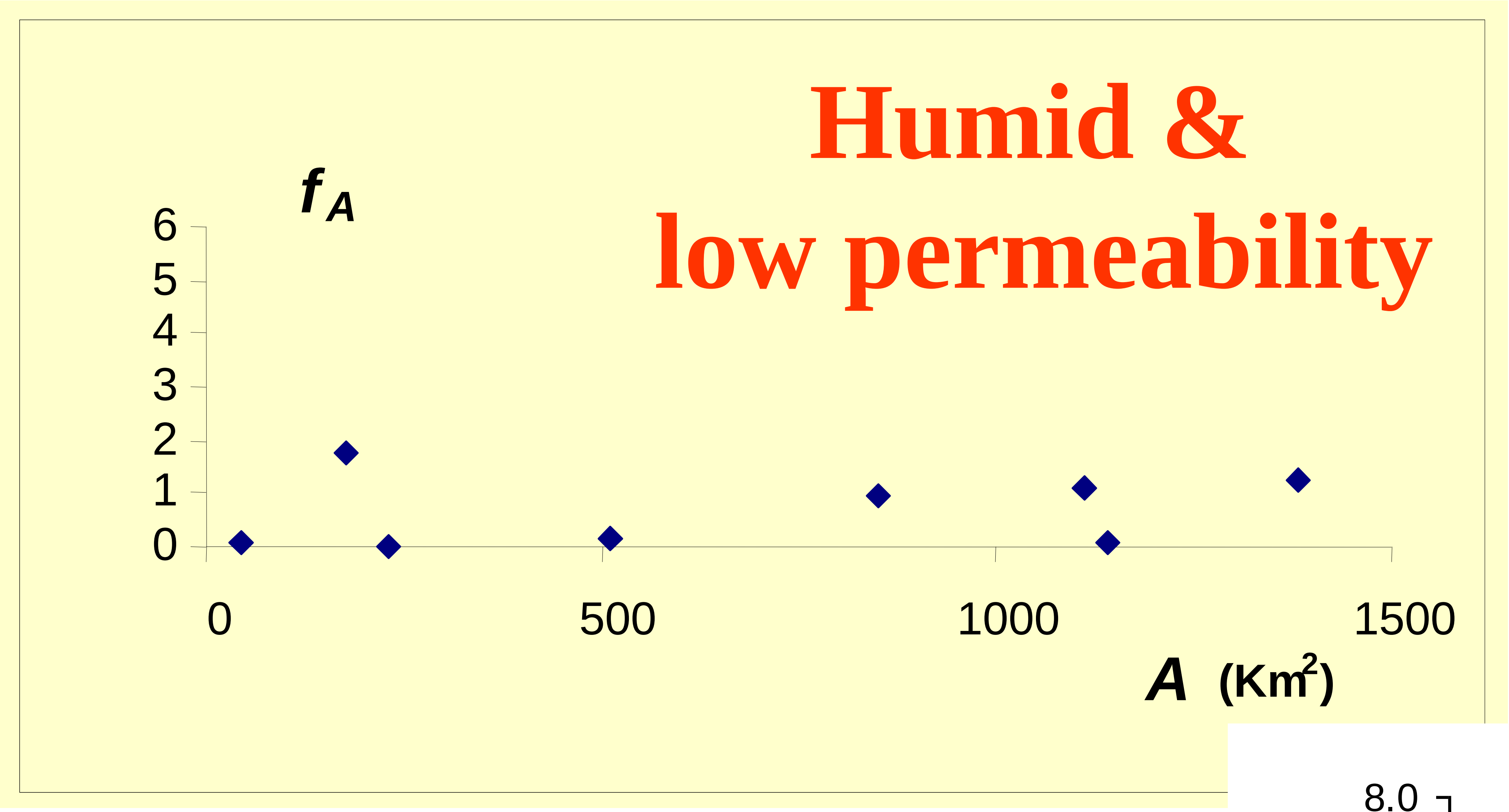

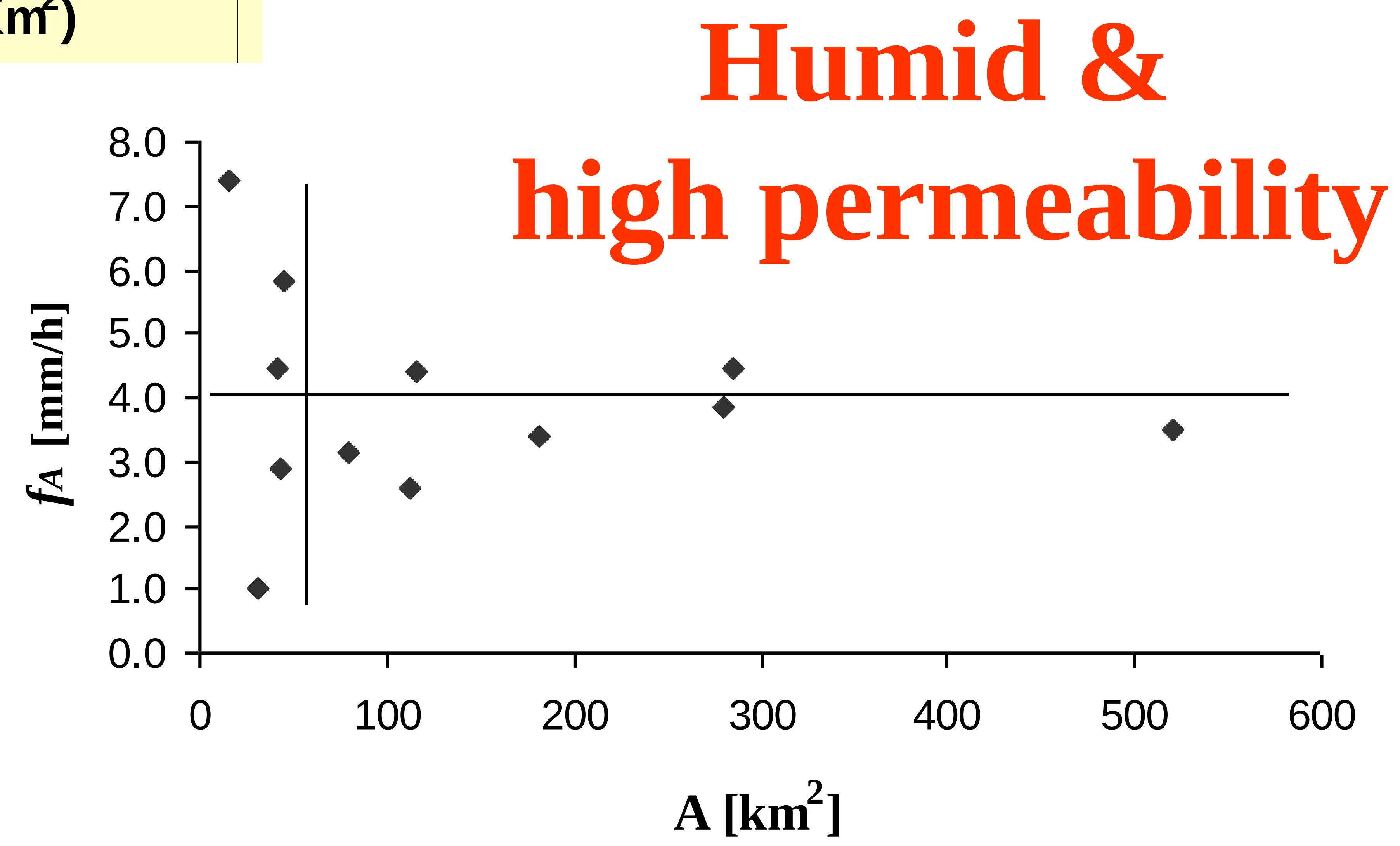

Model consistency: E[a]

Semi Arid Climate

In arid climate the mean contributing area was found to depend on the permeability (Fiorentino et al., 2001)

.

$r = -0.69\ \psi + 0.79,\ \ R^2=0.84$

$0.1 < r < 0.7$

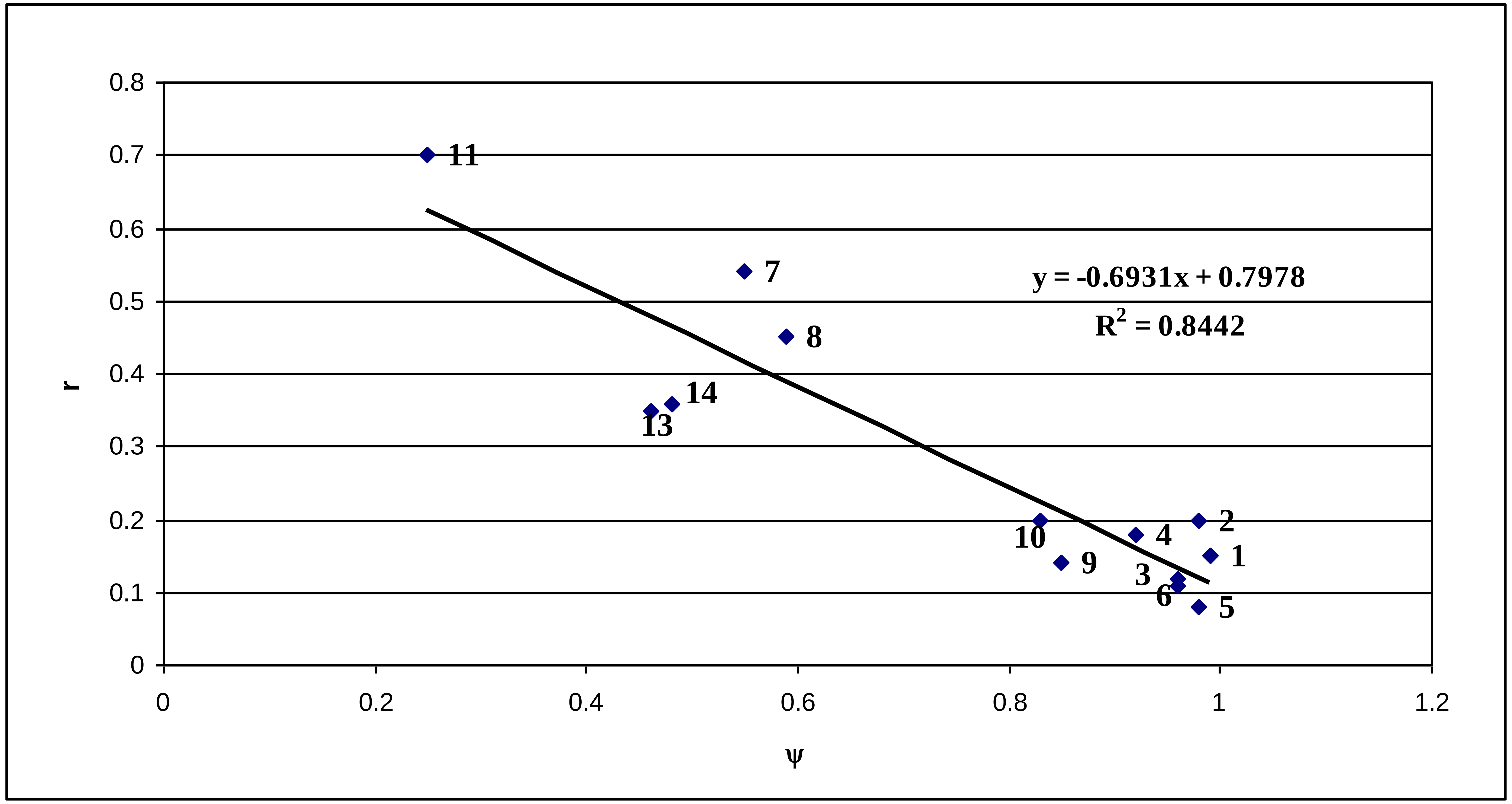

r = E[a]/ A

Model consistency: E[a]

Humid climate

In humid climate the mean contributing area was found to depend on the variation coefficient of the topographic index (Fiorentino et al. 2002).

$$r = 1.9\,Cv_I - 0.55,\quad R^2=0.90$$

$$0.15 < r < 0.3$$

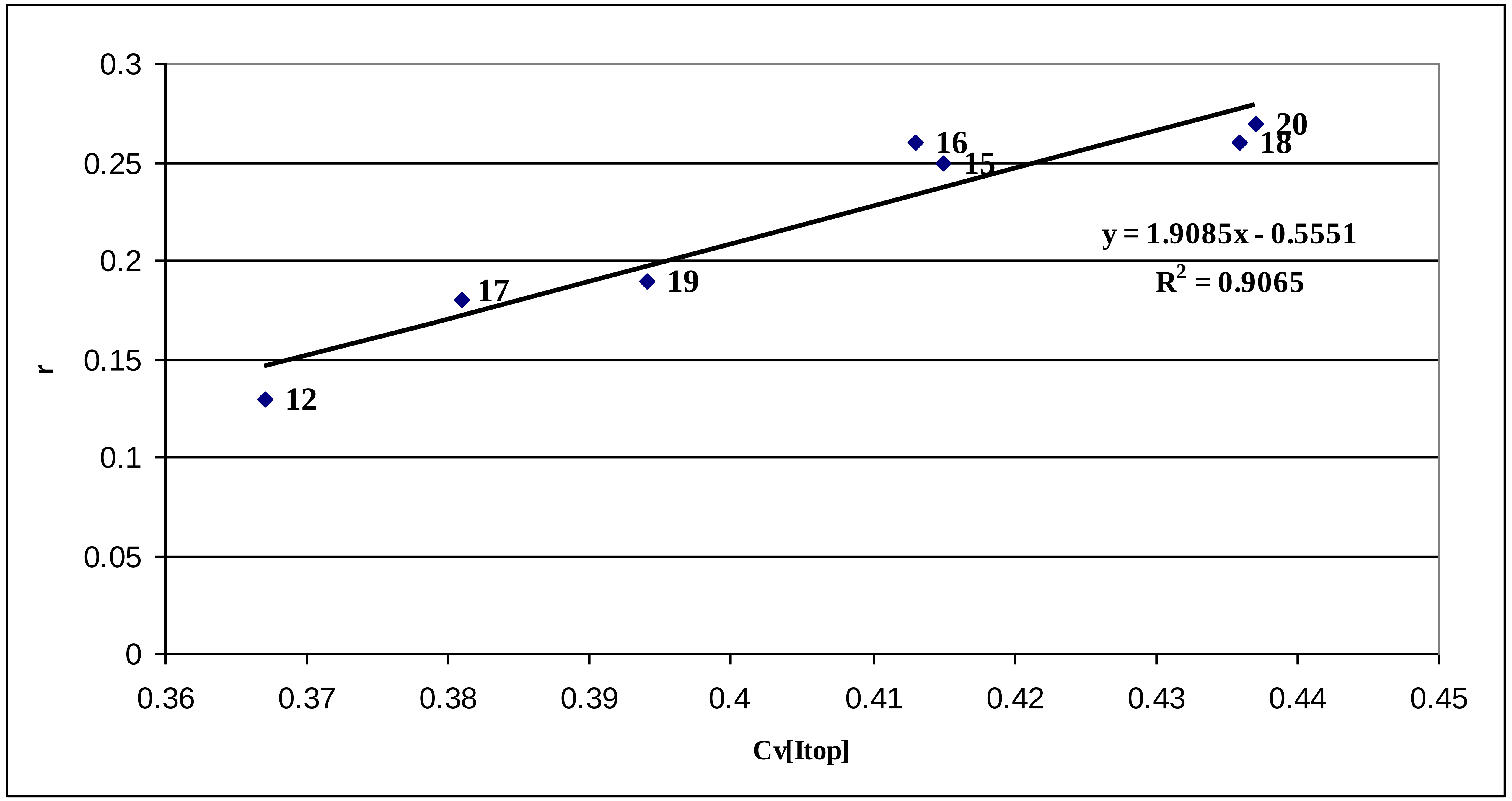

$$I_{Top} = \ln\left(\frac{a}{\tan(\beta)}\right)$$

Model consistency: Hydrological losses

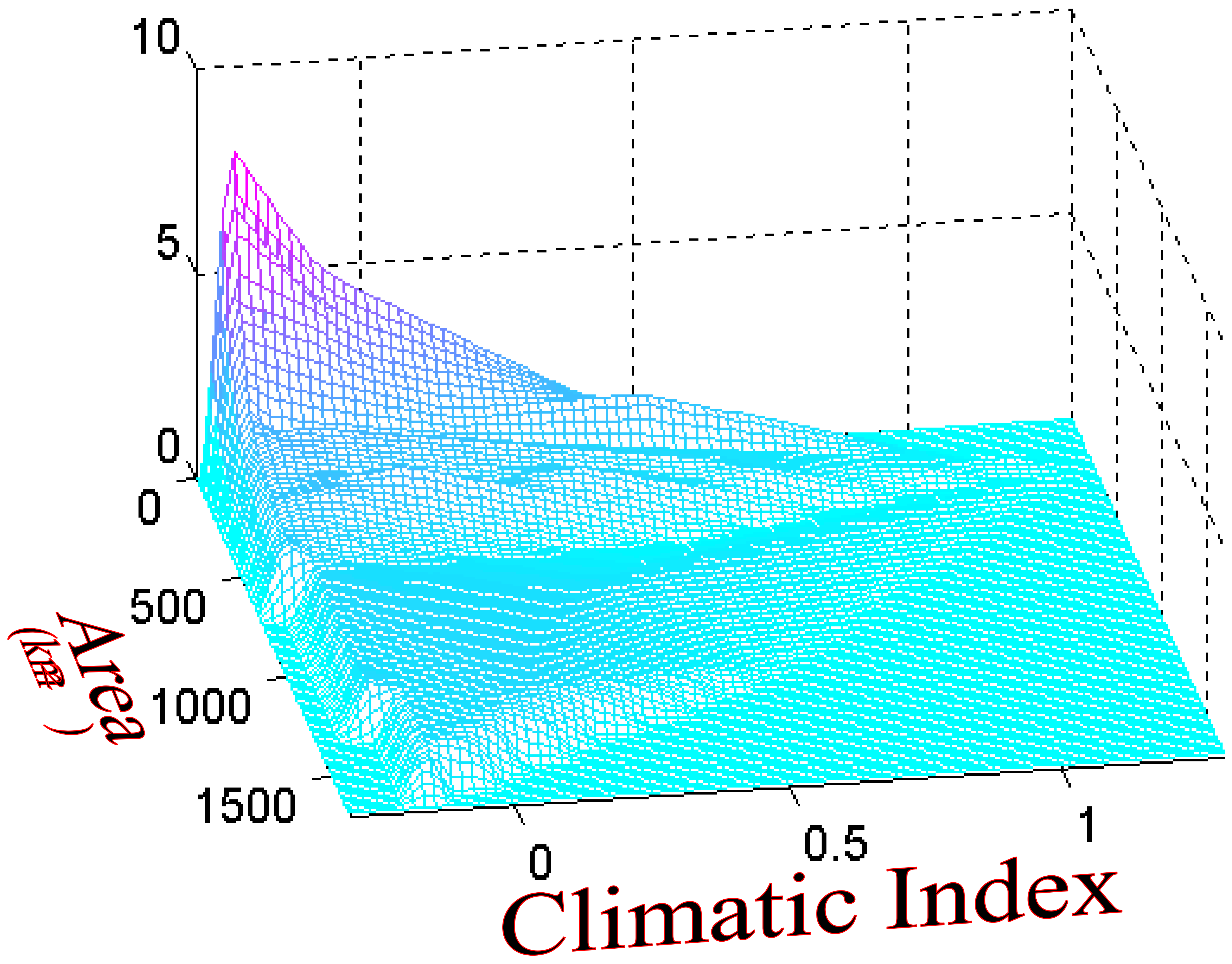

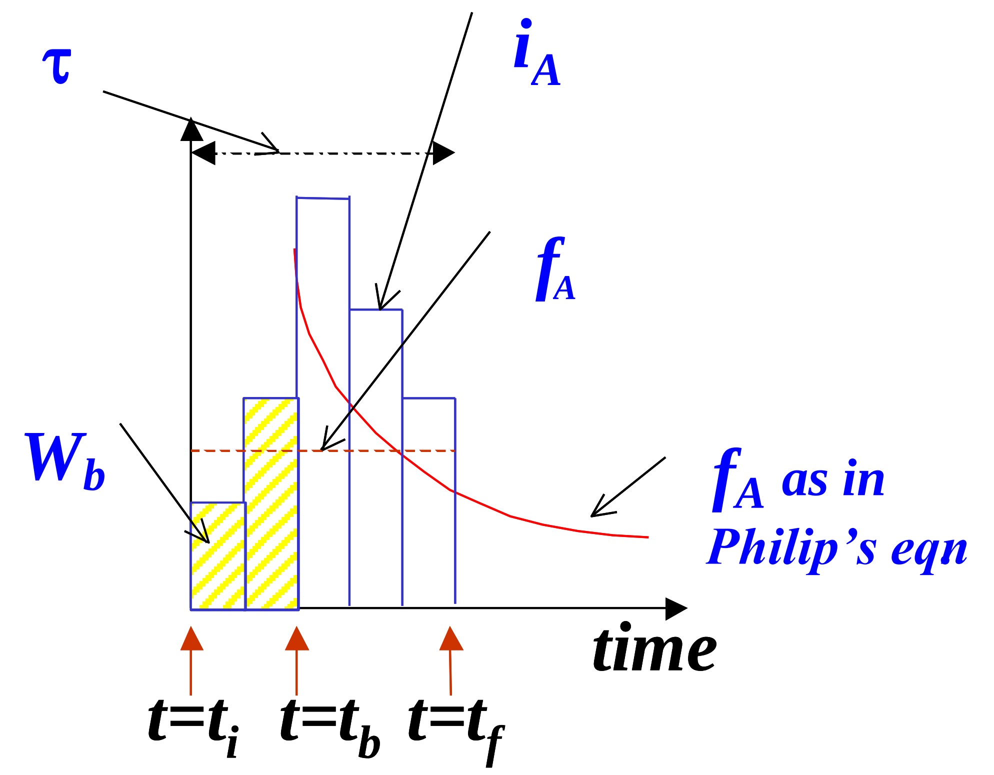

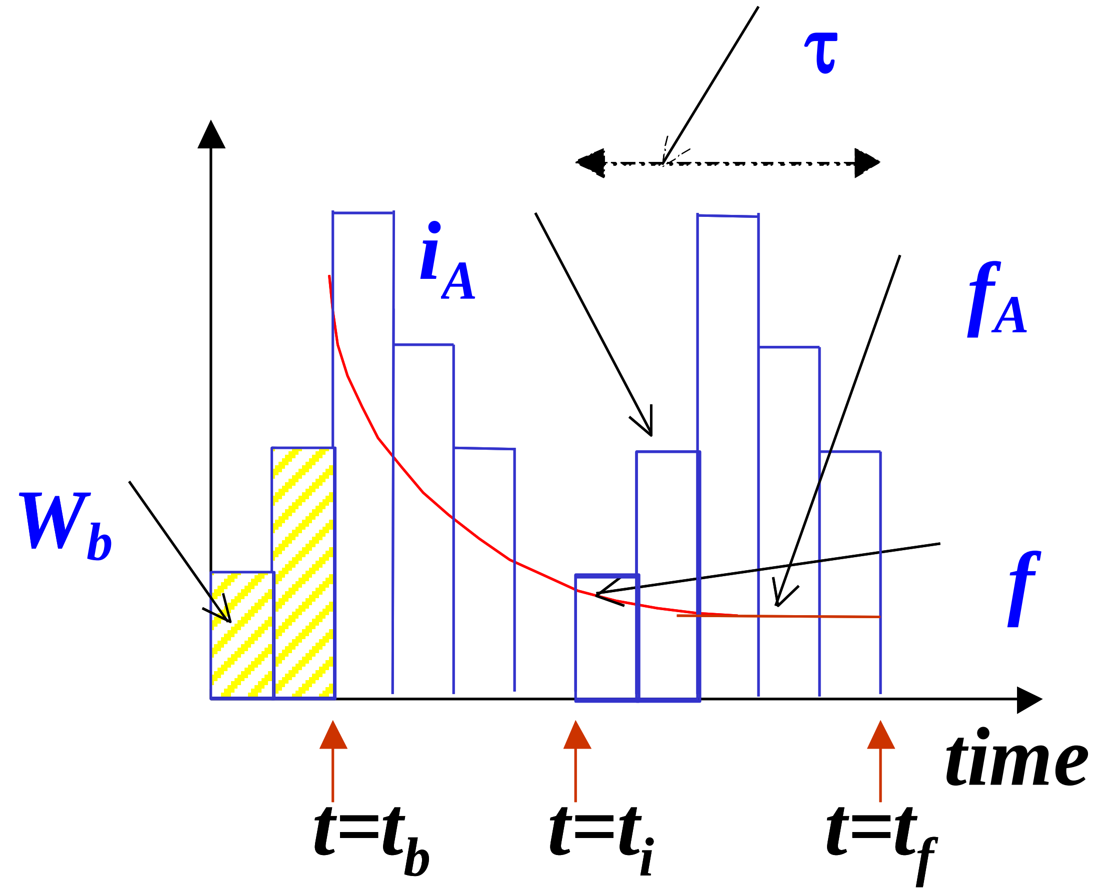

Un caso di studio: individuazione del modello

nta Maria at Ponte Lucera Torremaggio	1
Triolo at Ponte Lucera Torremaggiore	2
Salsola at Ponte Foggia San Severo	3
Casanova at Ponte Lucera Motta	4
Celone at Ponte Foggia San Severo	5
Celone at San Vincenzo	6
Cervaro at Incoronata	7
Carapelle at Carapelle	8
Venosa at Ponte Sant' Angelo	9
Arcidiaconata at Ponte Rapolla Lavello	10
Ofanto at Rocchetta Sant' Antonio	11
Atella at Ponte sotto Atella	12
Bradano at Ponte Colonna	13
Bradano at San Giuliano	14
Basento at Pignola	15
Basento at Gallipoli	16
Basento at Menzena	17
Agri at Tarangelo	18
Sinni at Valsinni	19
Sinni at Pizzutello	20
Crati at conca	21
Esaro at La musica	22
Coscile at Camerata	23
Trionto at Difesa	24
Tacina at Rivioto	25
Alli at Orso	26
Melito at Olivella	27
Corace at Grascio	28
Ancinale at Razzona	29
Alaco at Mammone	30
Amato at Marino	31
Lao at piè di Borgo	32
Noce at la Calda	33

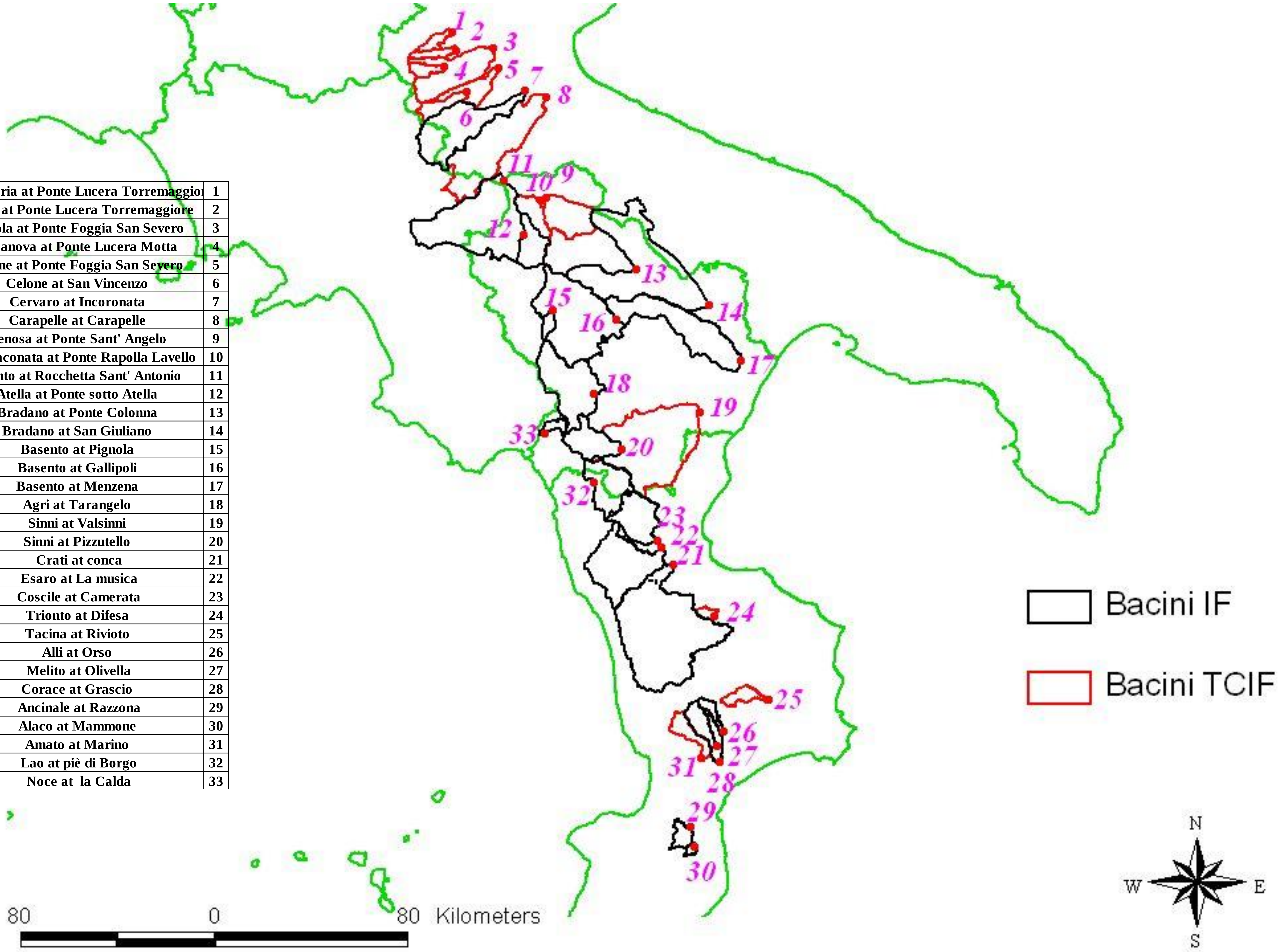

Il clima

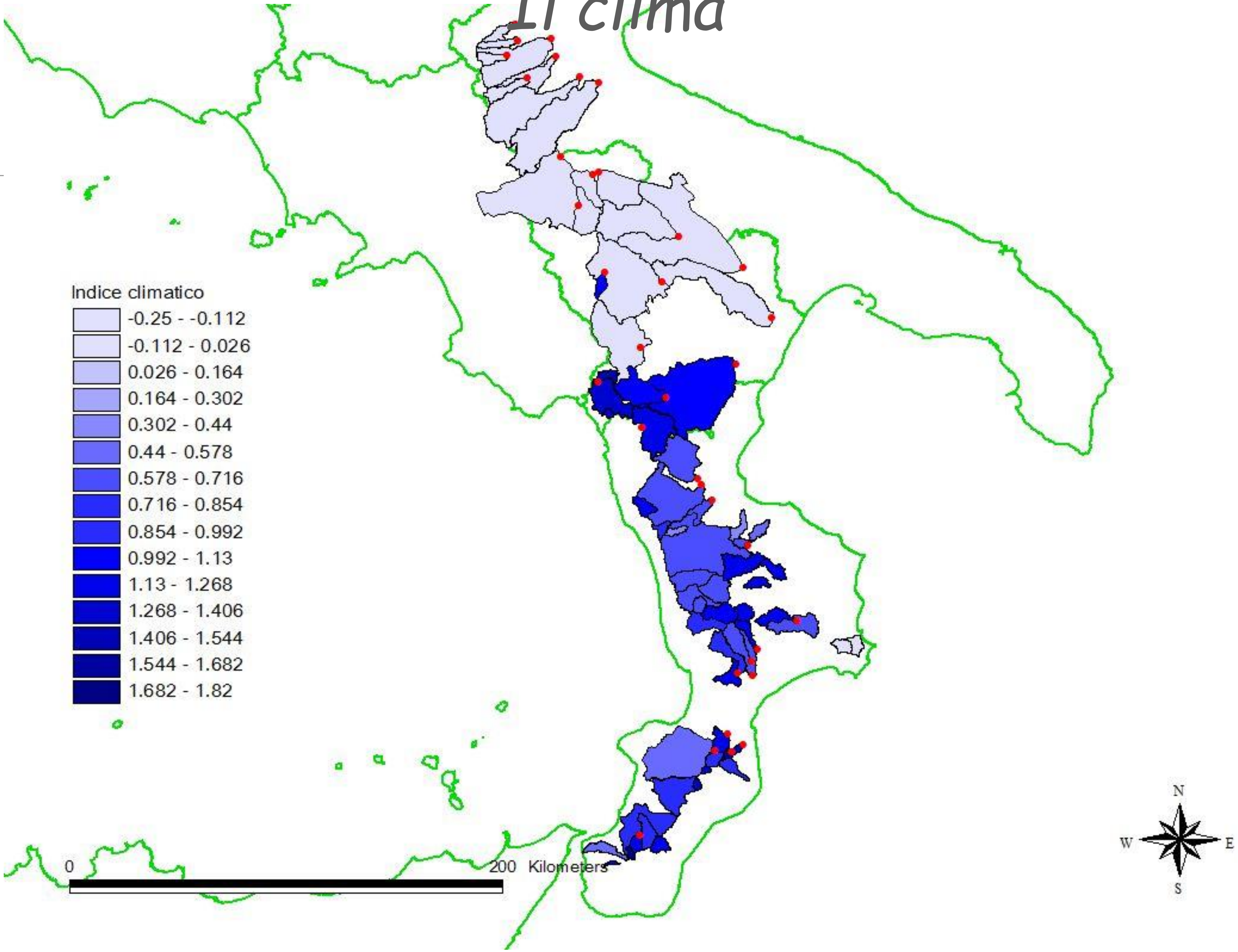

Indice climatico
-0.25 - -0.112
-0.112 - 0.026
0.026 - 0.164
0.164 - 0.302
0.302 - 0.44
0.44 - 0.578
0.578 - 0.716
0.716 - 0.854
0.854 - 0.992
0.992 - 1.13
1.13 - 1.268
1.268 - 1.406
1.406 - 1.544
1.544 - 1.682
1.682 - 1.82
0
200 Kilometers
N
W
E
S

La verifica del modello regionale

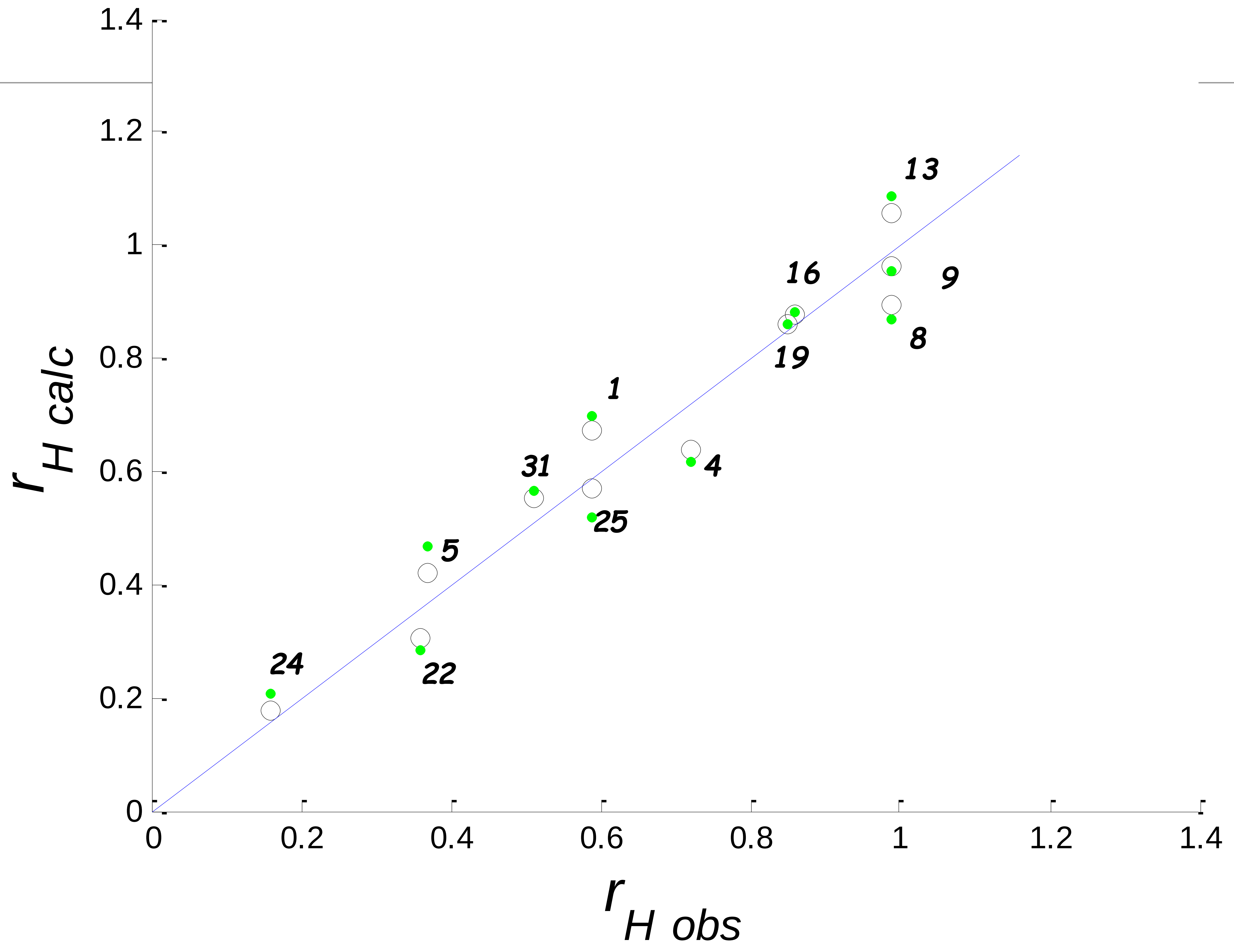

Risultati

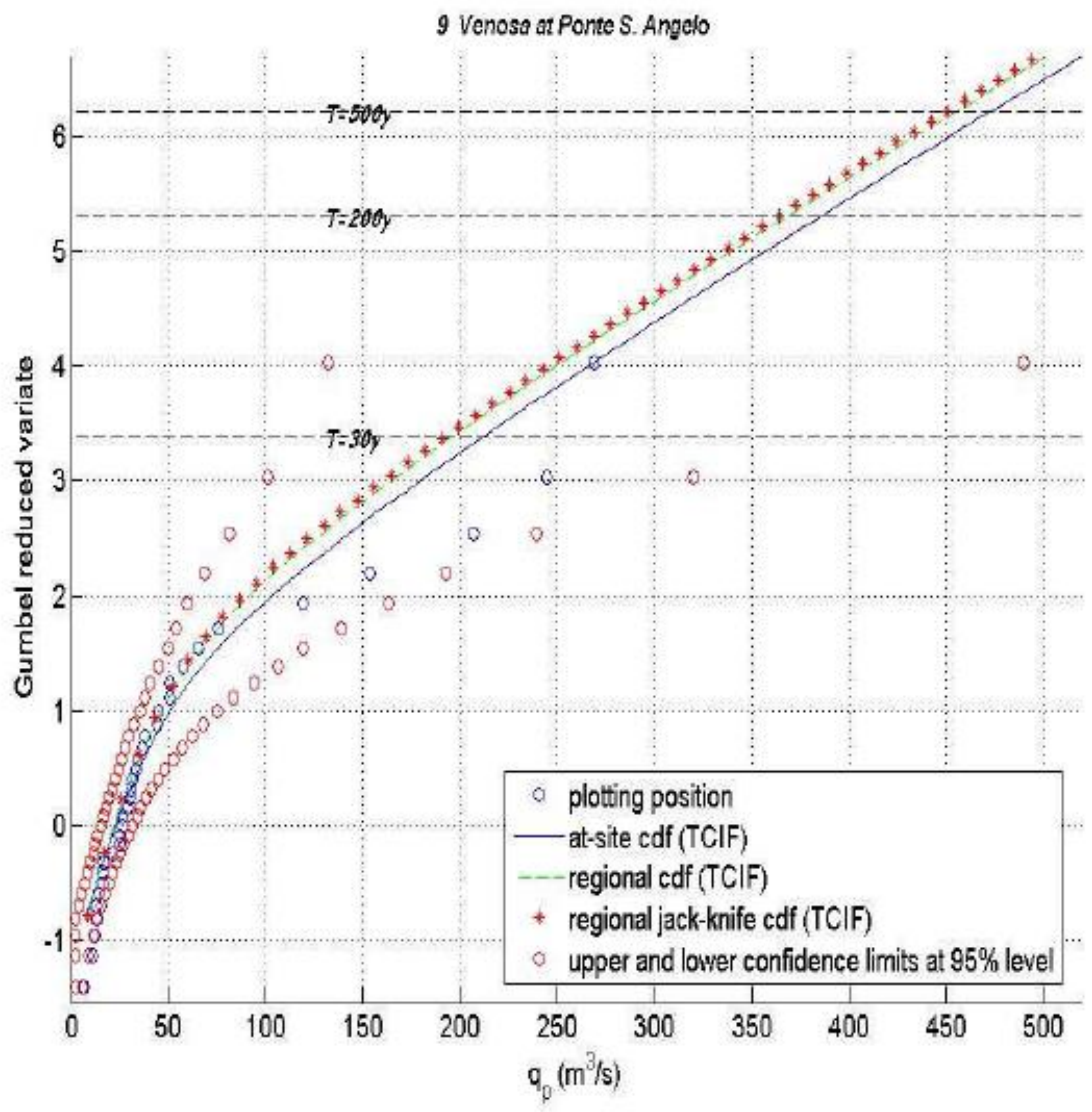
9 Venosa at Ponte S. Angelo
T=500y
T=200y
T=30y
Gumbel reduced variate
q_p (m³/s)
plotting position
at-site cdf (TCIF)
regional cdf (TCIF)
regional jack-knife cdf (TCIF)
upper and lower confidence limits at 95% level

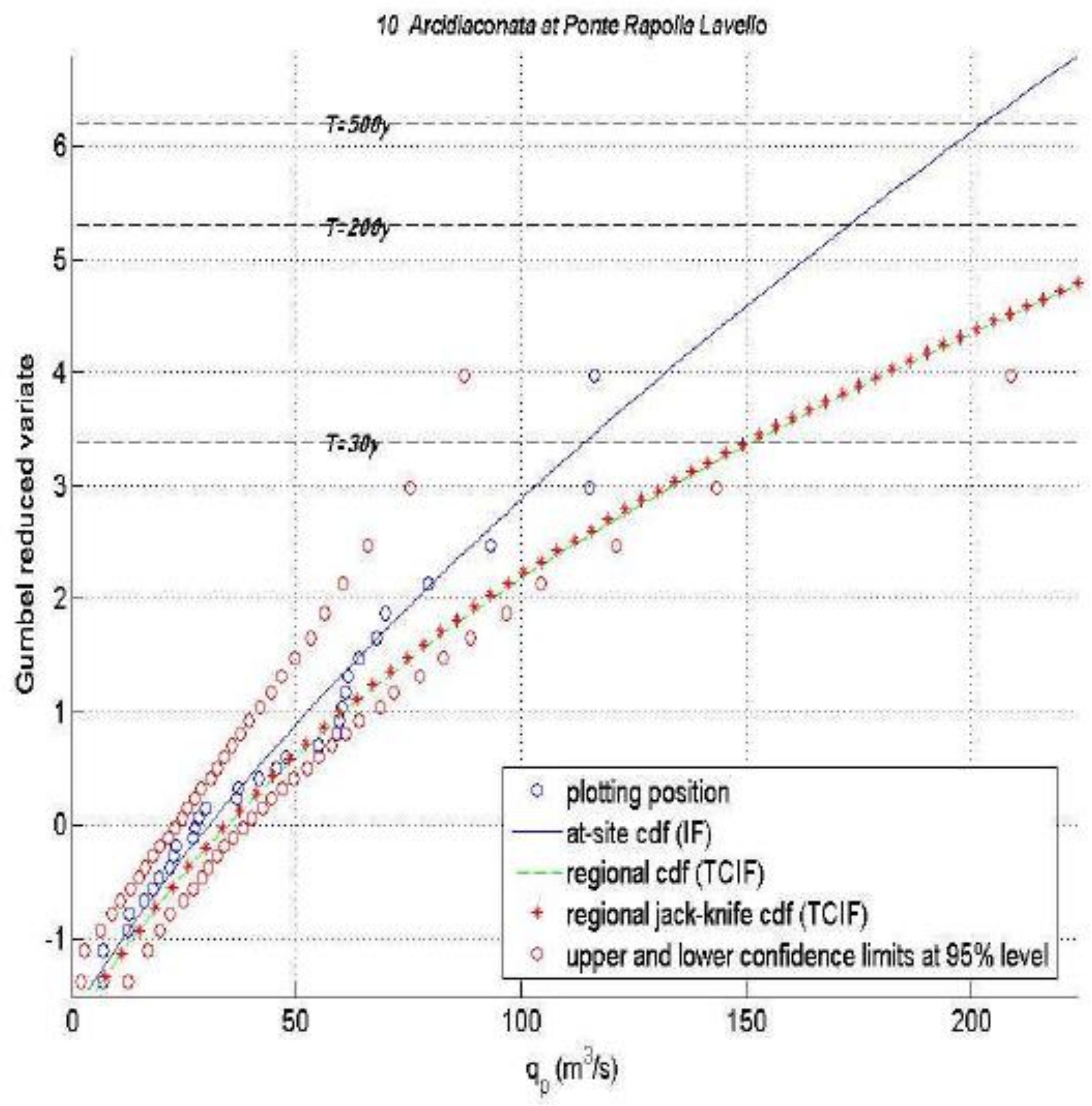
10 Arcidiaconata at Ponte Rapolla Lavello
T=500y
T=200y
T=30y
Gumbel reduced variate
q_p (m³/s)
plotting position
at-site cdf (IF)
regional cdf (TCIF)
regional jack-knife cdf (TCIF)
upper and lower confidence limits at 95% level

Risultati

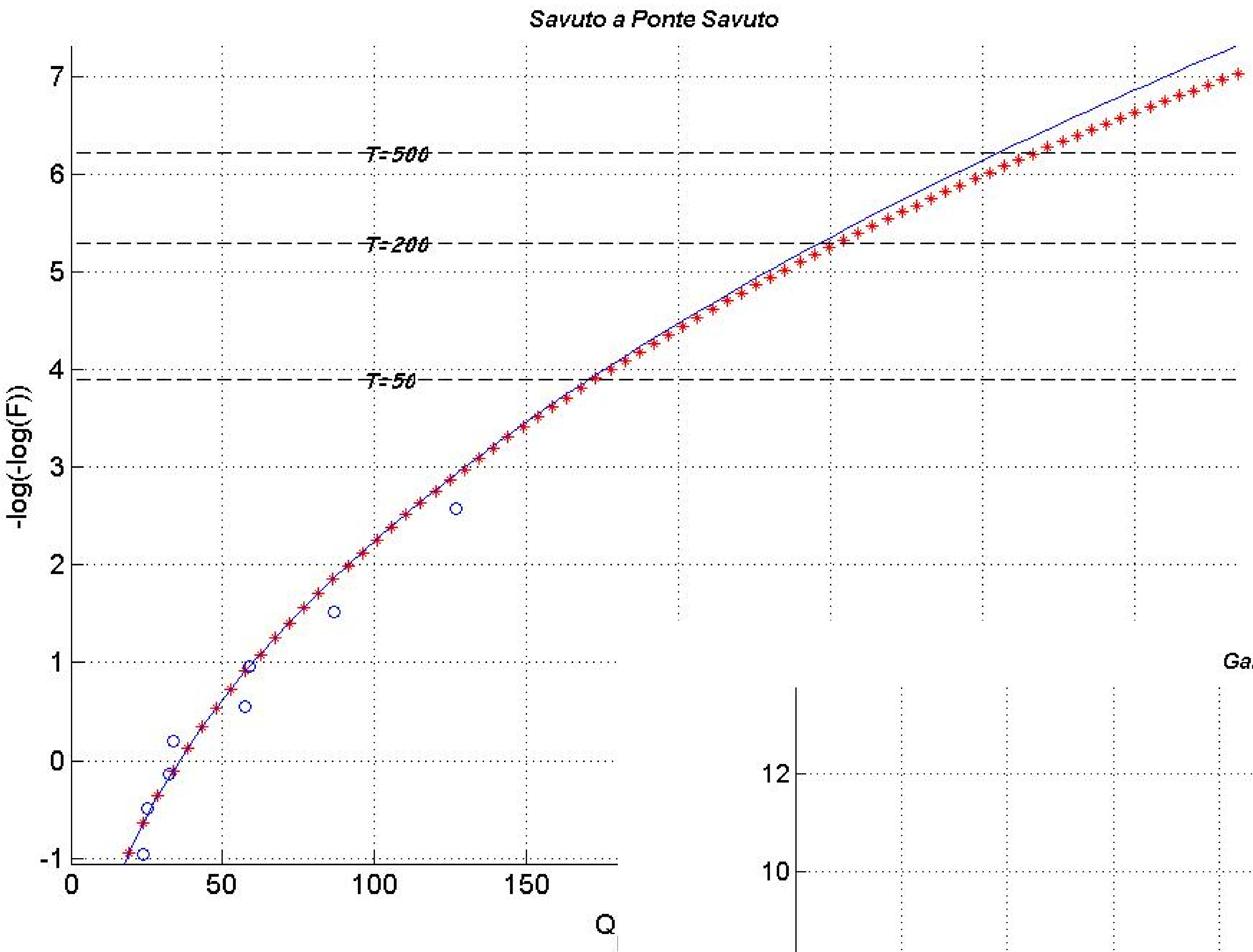
Savuto a Ponte Savuto
-log(-log(F))
Q
T=500
T=200
T=50

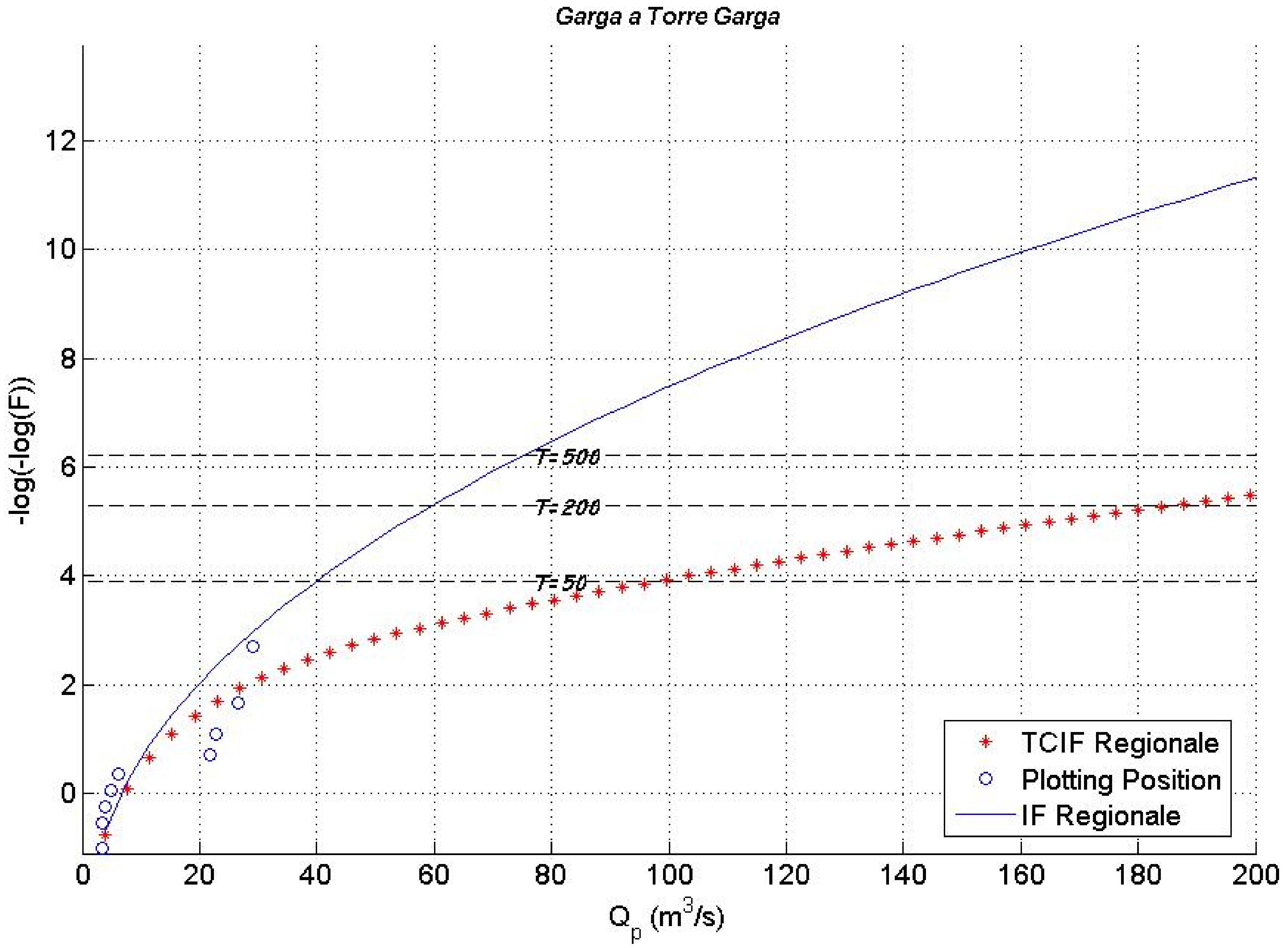
Garga a Torre Garga
-log(-log(F))
Q_p (m^3/s)
T=500
T=200
T=50
TCIF Regionale
Plotting Position
IF Regionale

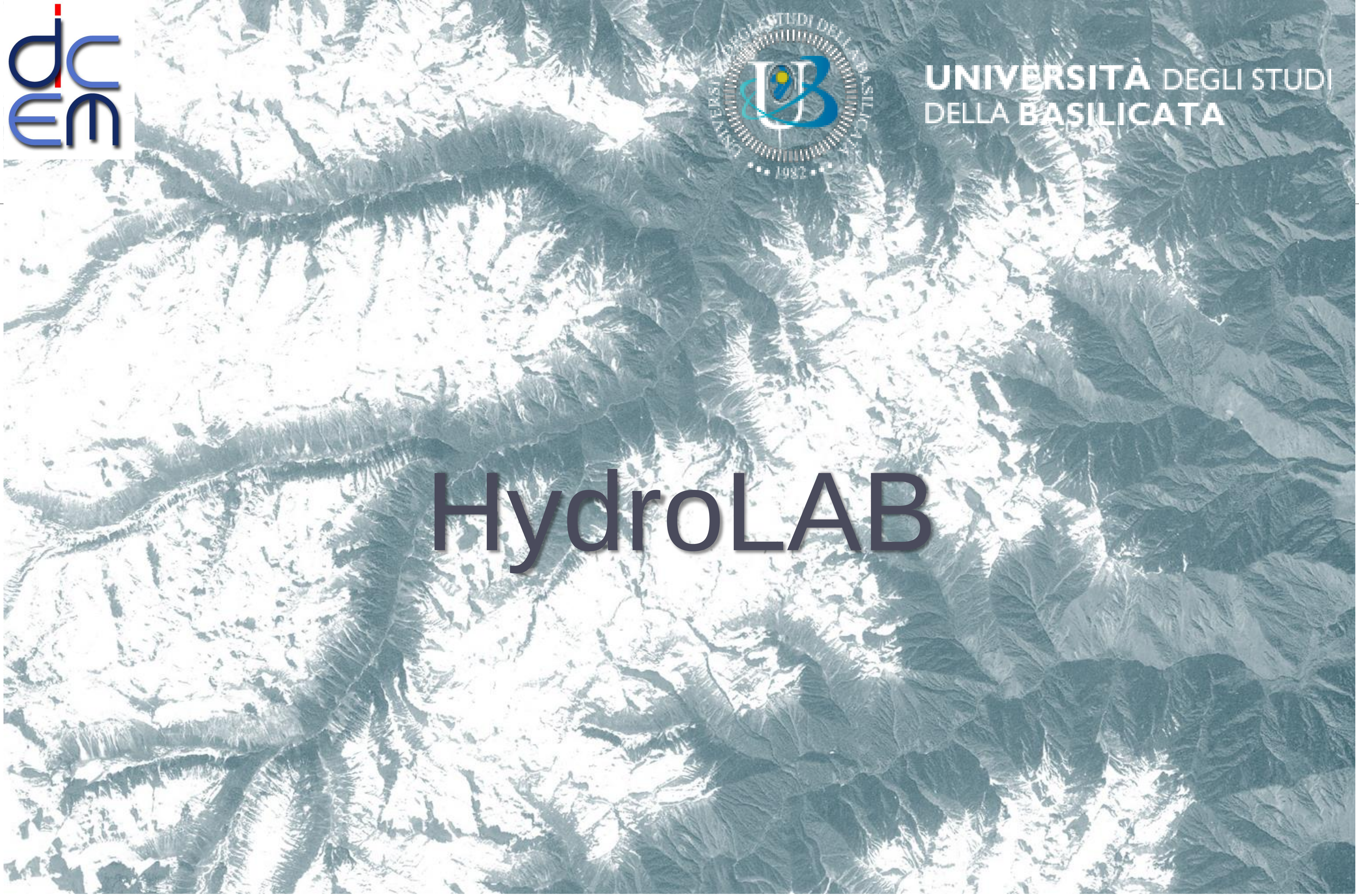

UNIVERSITÀ DEGLI STUDI DELLA BASILICATA

HydroLAB

HYDROLAB

HYDROLAB of the University of Basilicata has a group of researchers that cover a wide range of research activities in the field of Hydraulic Constructions, Hydraulics, hydrology and Ecohydrology.

HydroLAB

- Laboratory of Hydraulic Construction and Hydraulic
- GIS Laboratory
- Numerical Modelling LAB
- Techniques for the Management of River Basins

Field Measurements

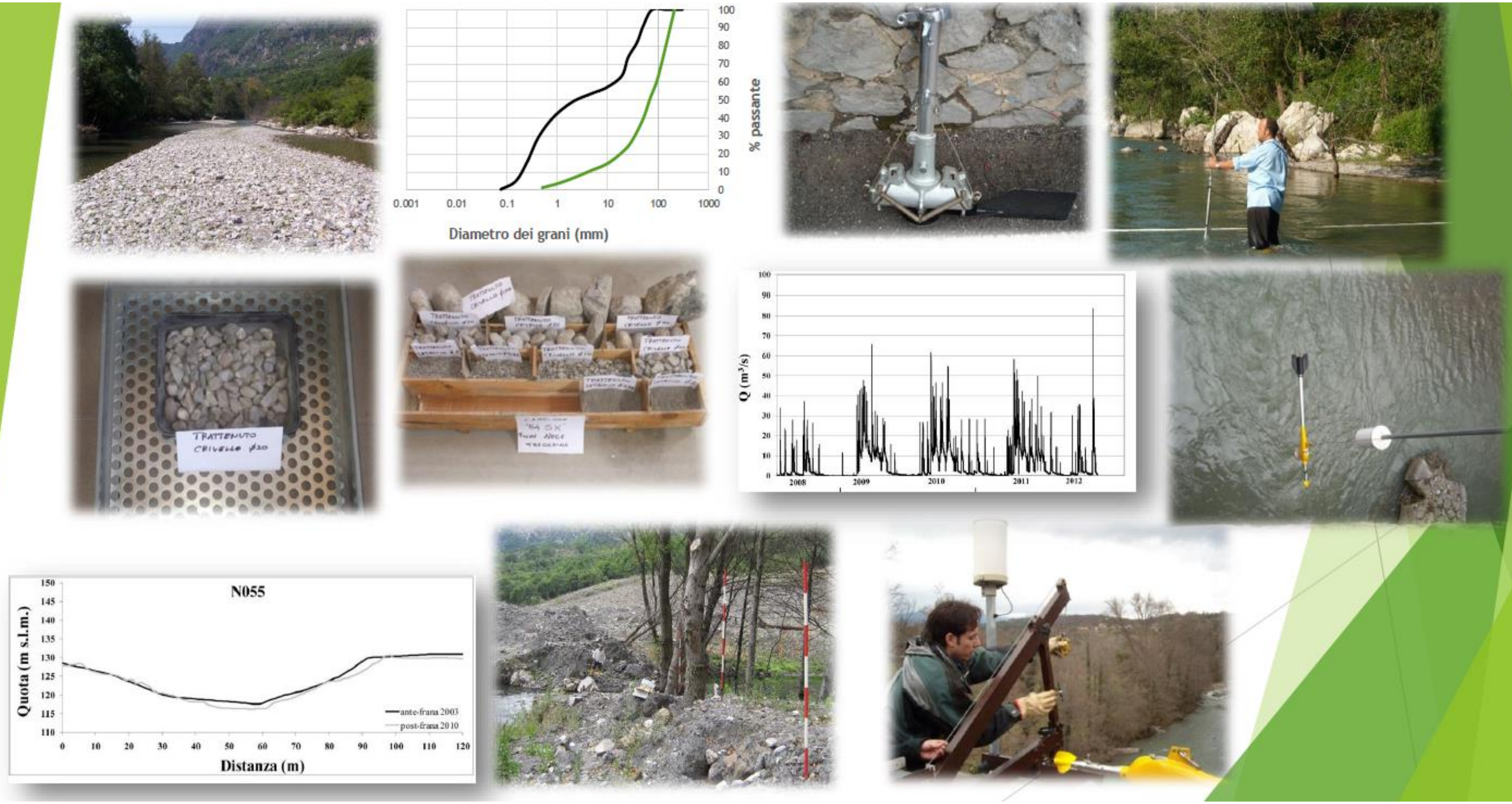

Hydrological Modeling

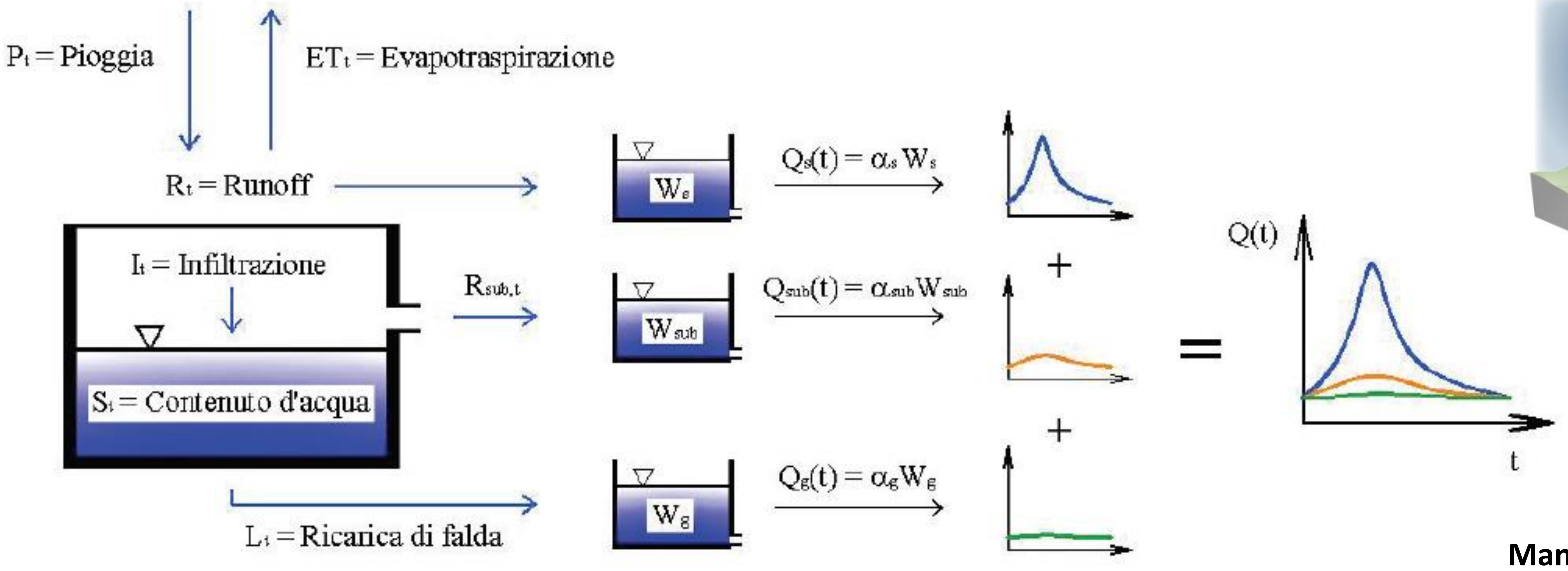

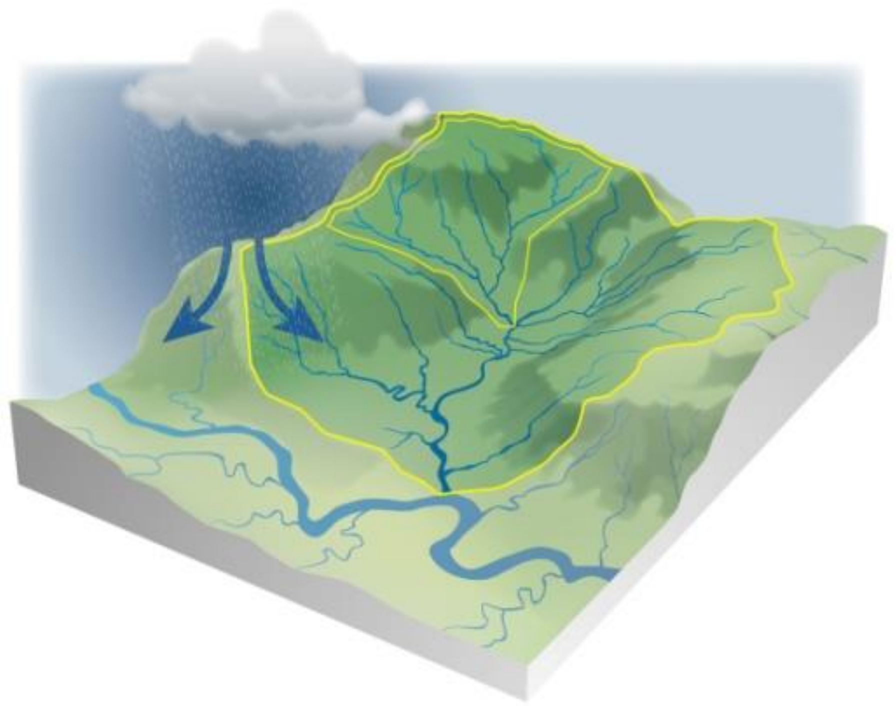

Manfreda & Fiorentino (2008)

AD2 (Aflussi-Deflussi 2)

- **Lumped model** with **physical based parameters**.

- AD2 has been applied for hydrological forecast (**meteo-hydrological**) with the advantage of a **limited number of parameters** and **reduced computational complexity**.

- the **calibration** of the model makes the model **versatile** for applications in **different environmental** and **climatic conditions**.

Distributed Modelling
DREAM

(Distributed model for Runoff, Evapotranspiration, and Antecedent soil Moisture simulation)

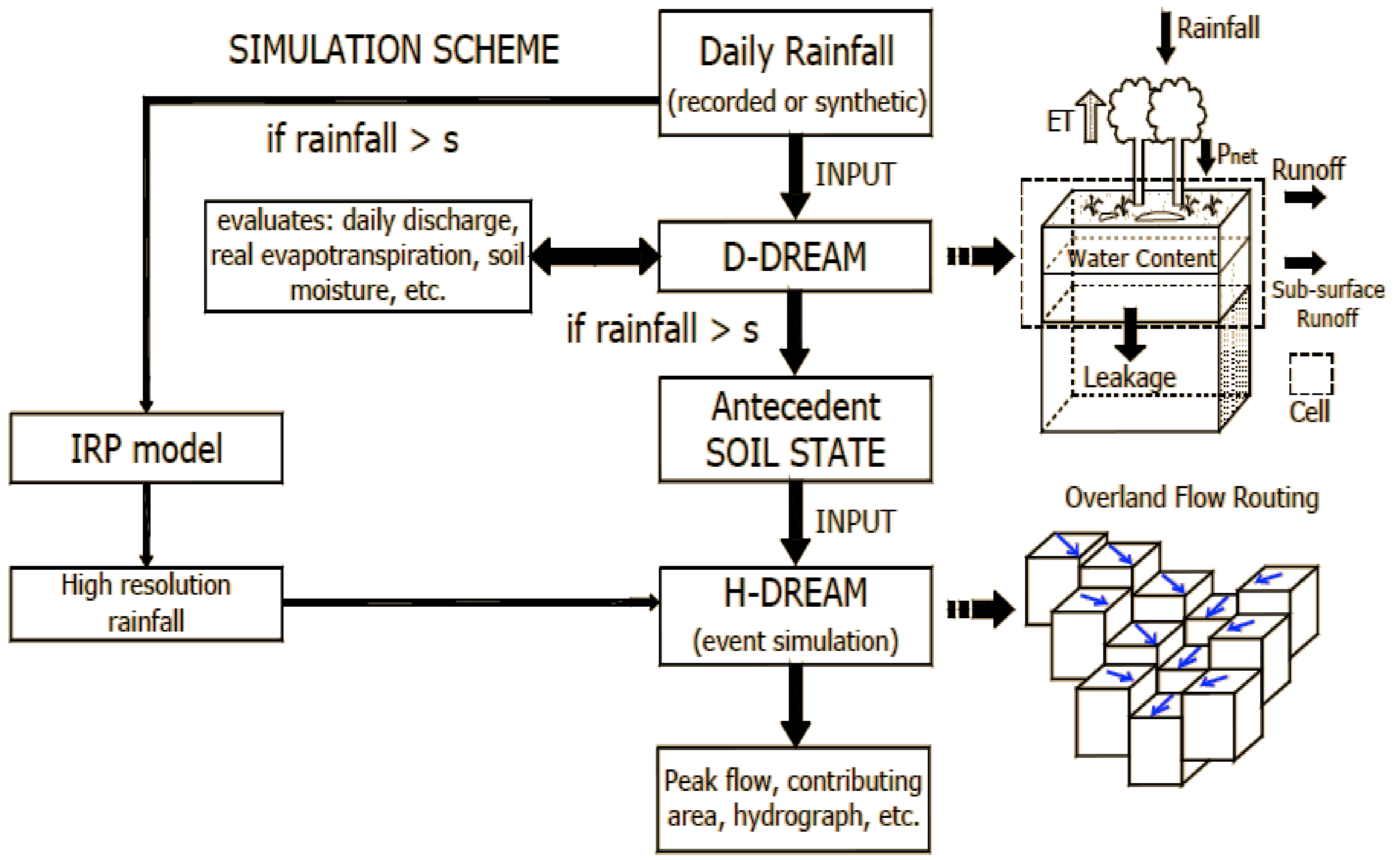

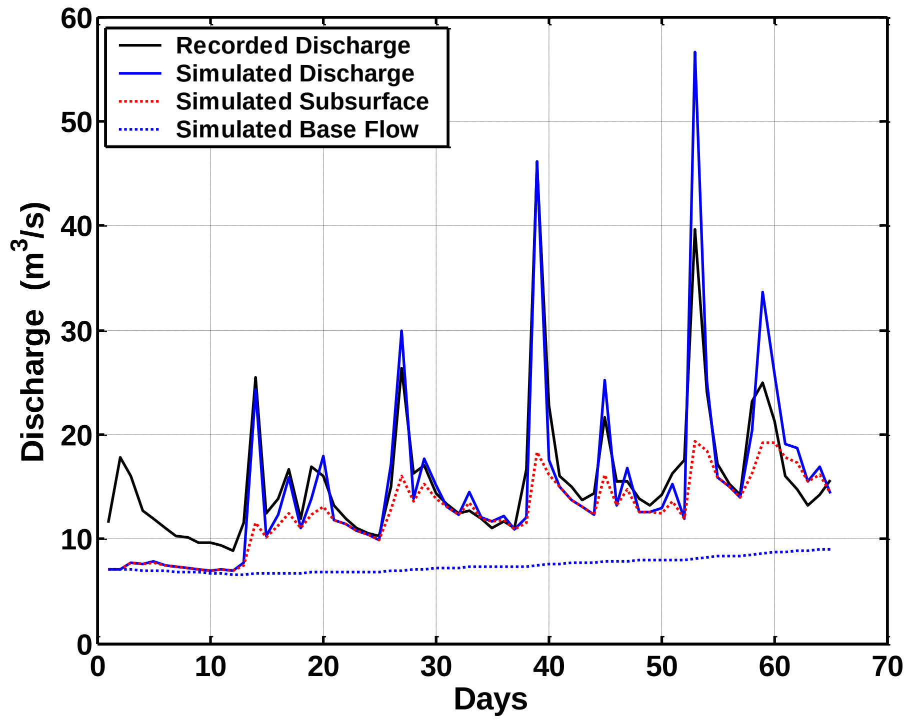

Manfreda et al. (ADGEO,2005)

- Takes into account the **spatial heterogeneity of hydrological variables** using **distributed data** contained in digital elevation models (DEMs), land use and soil texture maps.

- The model includes two sub-models operating at distinct time-scales.

- DREAM is a suitable model for the support of **integrated models for the prediction of flood events** that make use of forecasts obtained from models in global circulation and/or limited area

Hydropower Energy Optimization

SPR-IDRO^2

(Sistemi di PRevisione IDROlogica per la gestione di impianti IDROelettrici ad acqua fluente)

software platform that couples a meteorological model with a hydrological model in order to create tools needed to optimize the production of electricity from reservoirs and river plants. This tool will be able to provide a forecast on the potential production of energy at 24-48-72 hours.

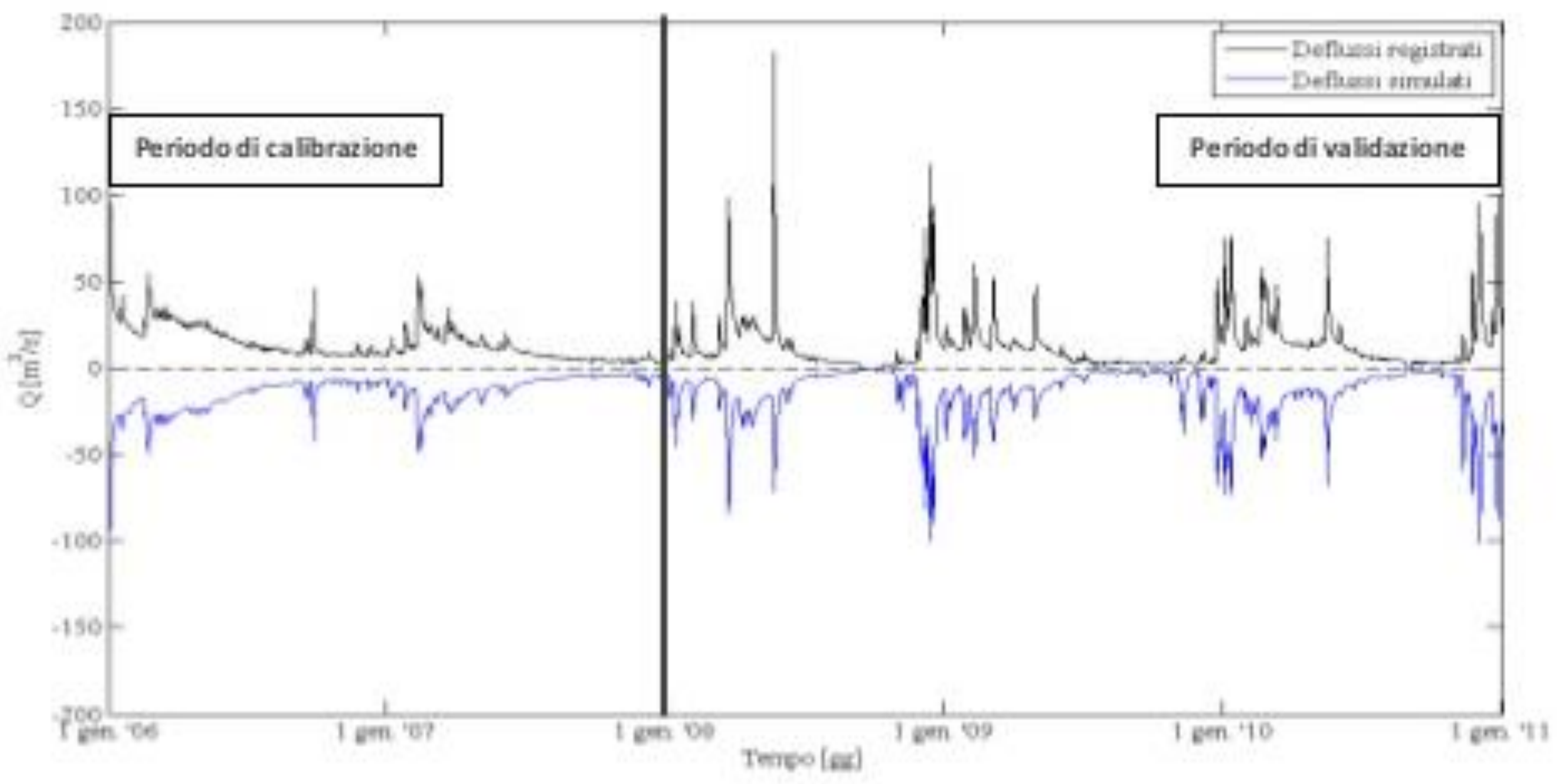

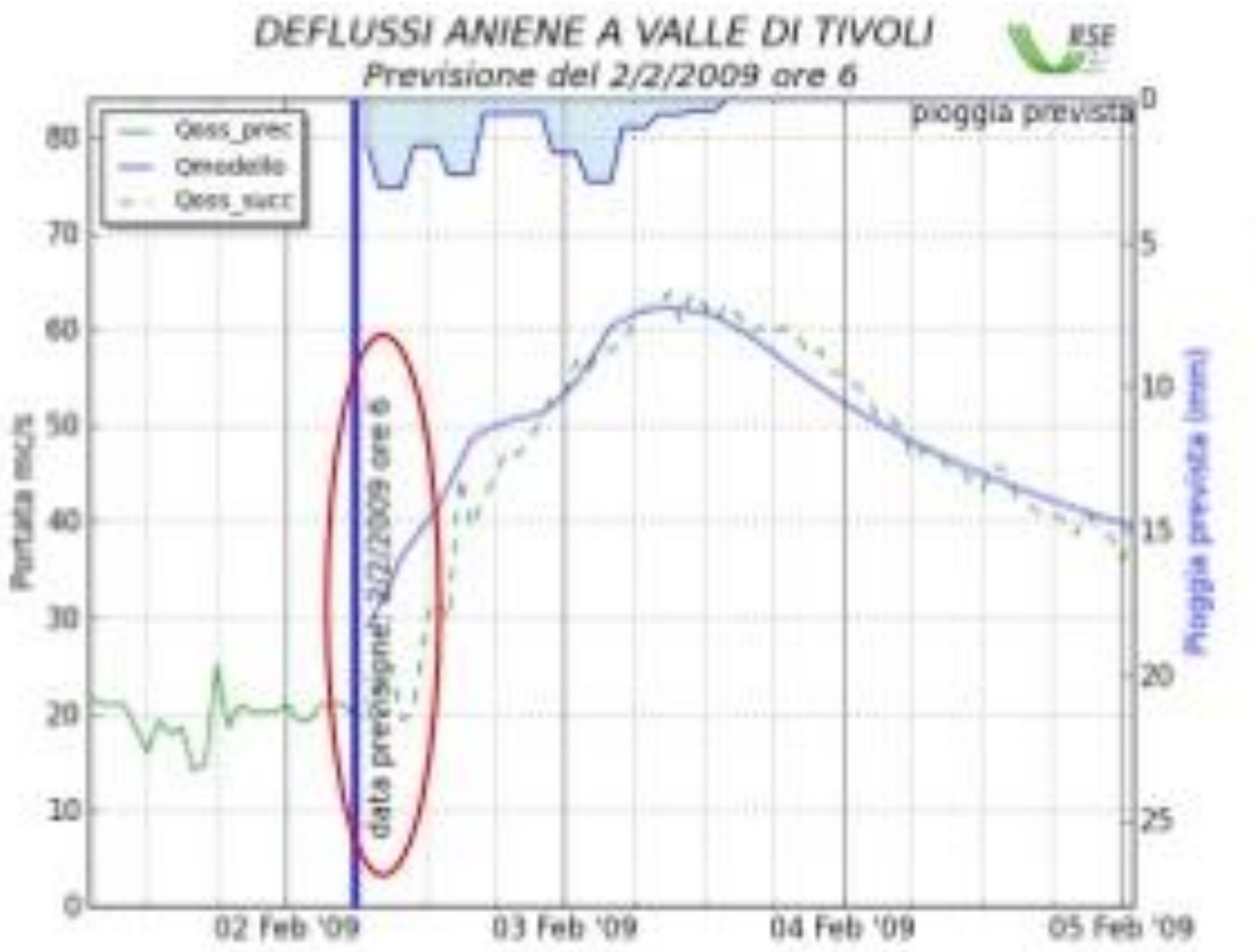

Manfreda e Mancusi (2013)

Geomorphic Approaches for the Delineation of Flood Prone Areas

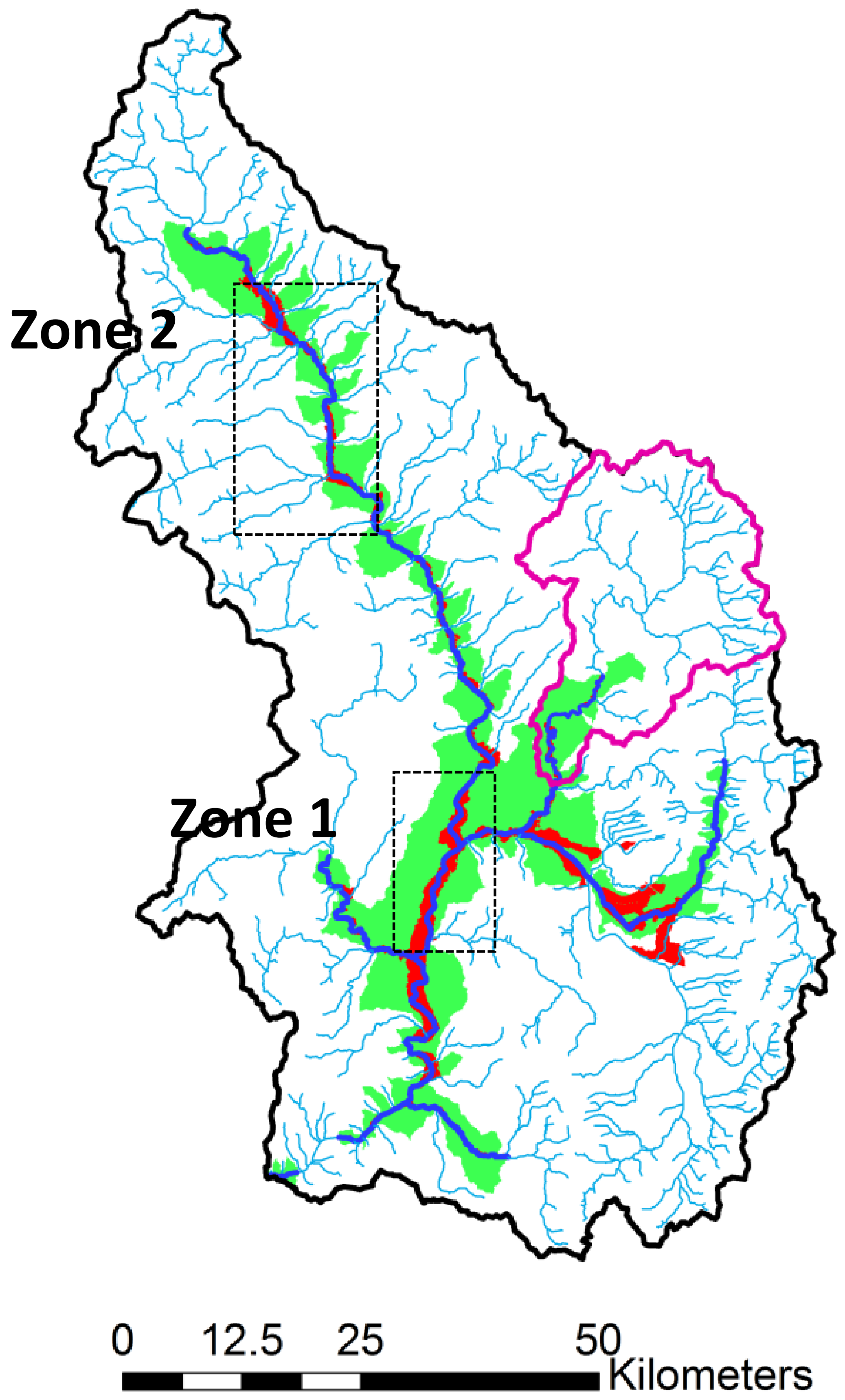

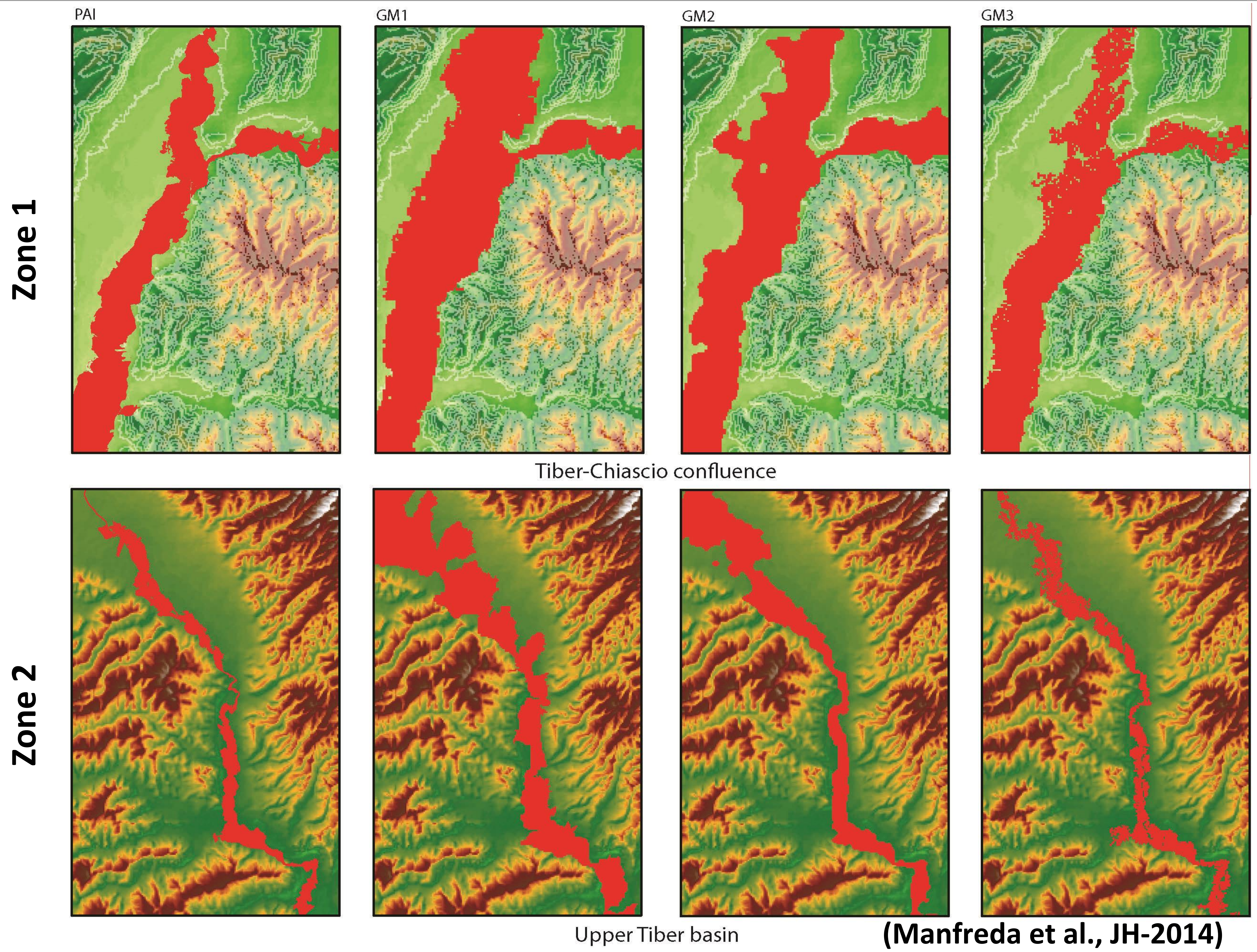

(Manfreda et al., JH-2014)

Advances in Hydraulic Modeling and Flood Impact

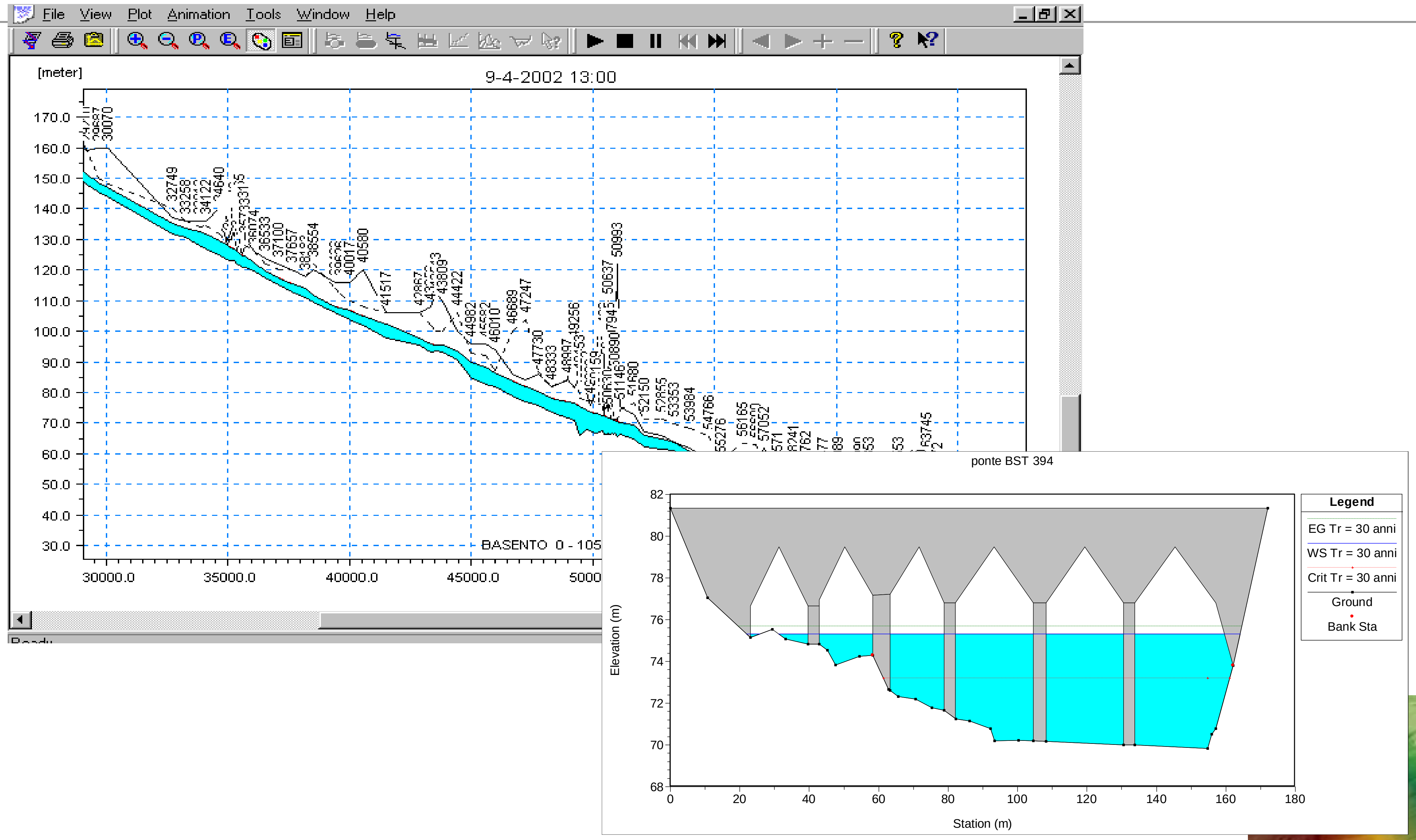

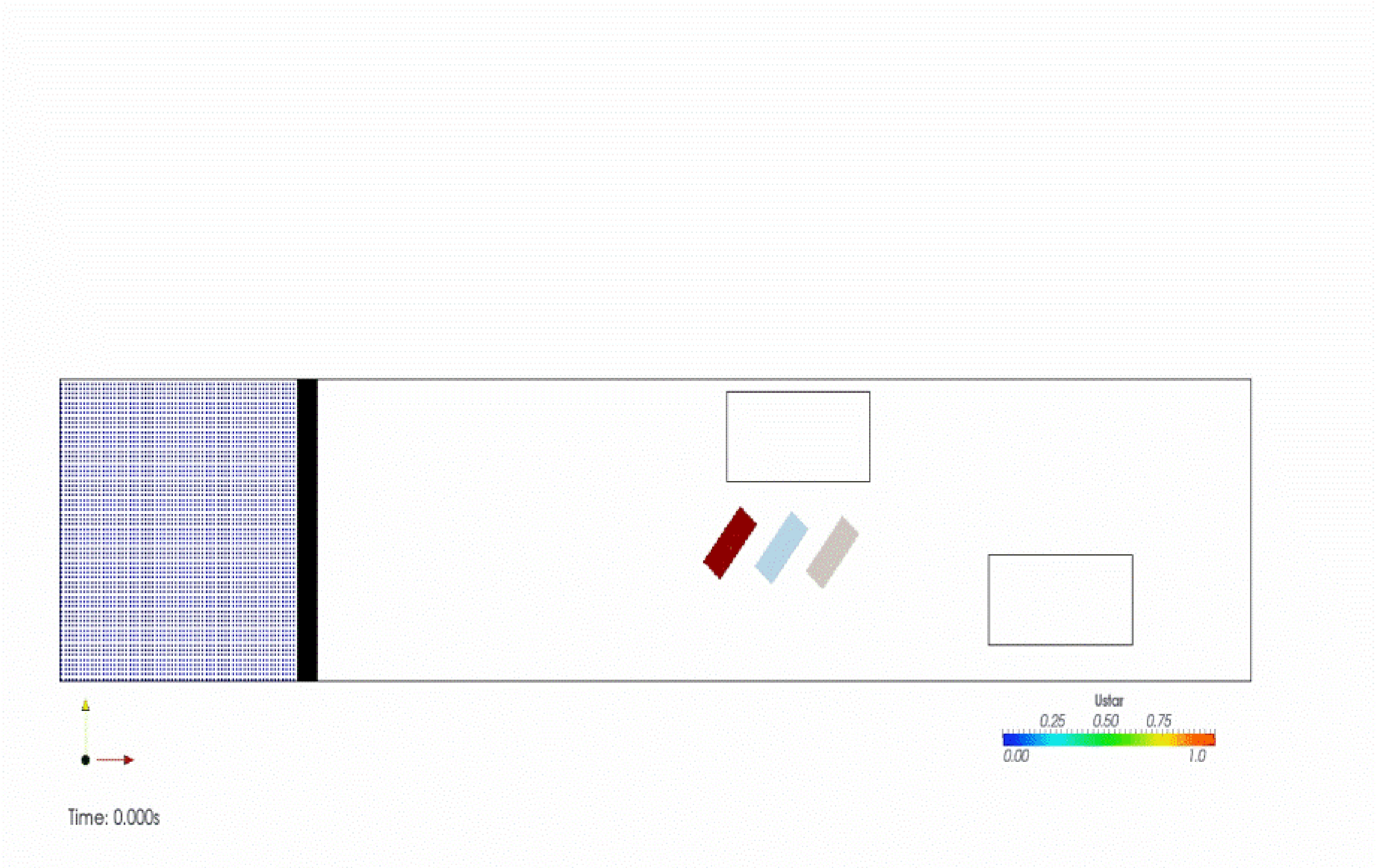

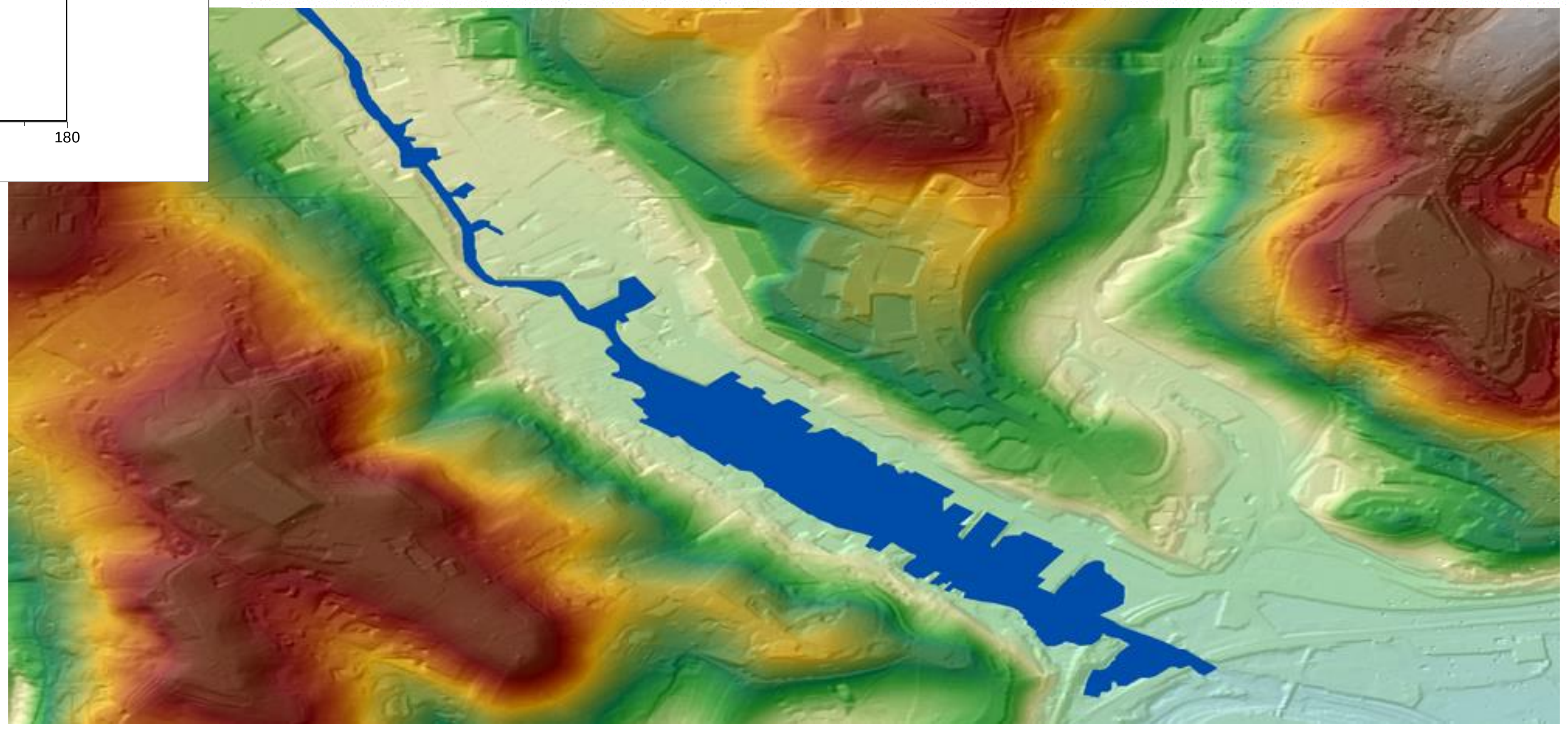

(Albano et al., in press 2014)

(Sole et al., 2013)

Soil Moisture Monitoring

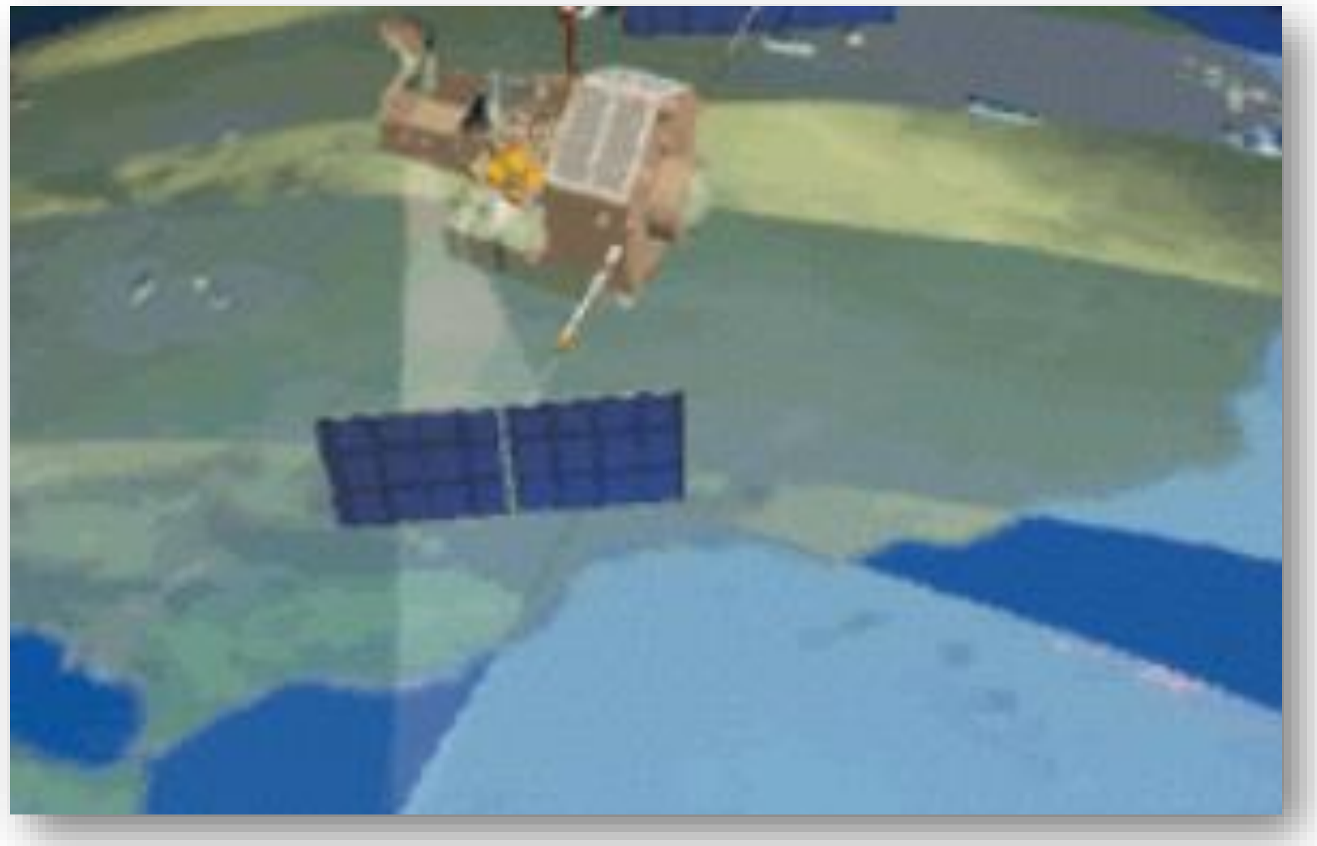

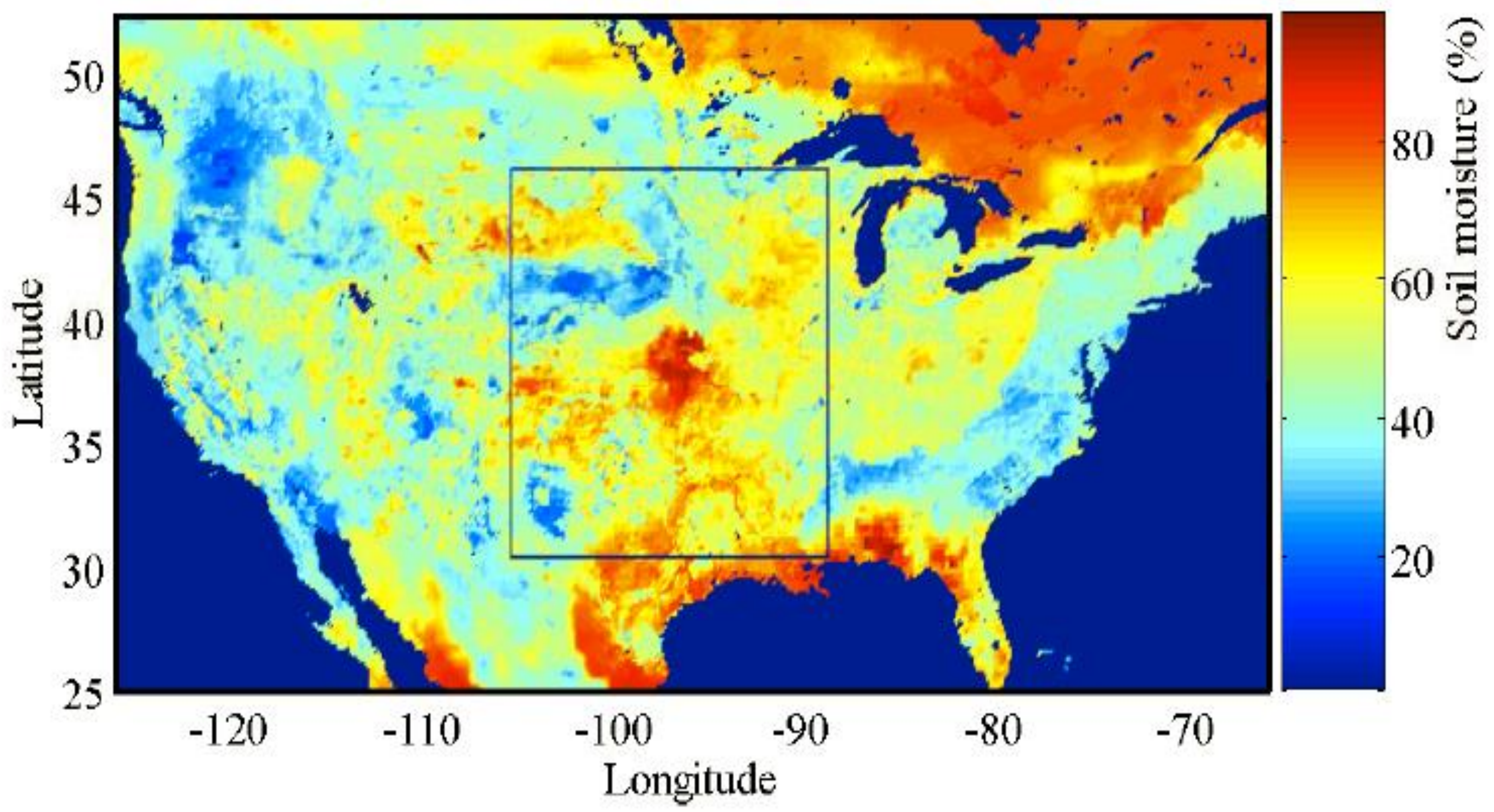

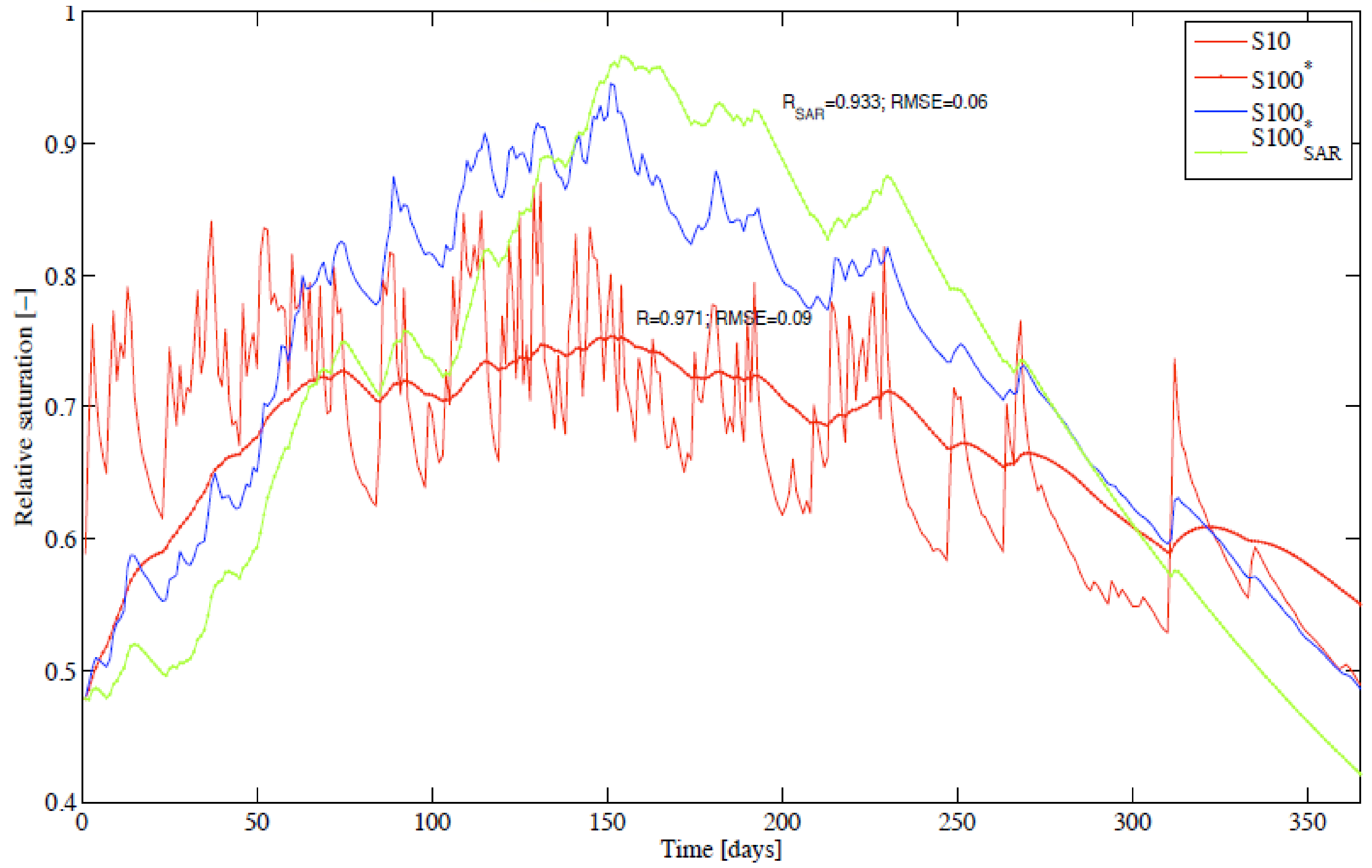

SMAR (Soil moisture analytical relationship)

- describes analytically the relation between surface soil moisture and the moisture of the root zone on the basis of time series of surface soil moisture data acquired by satellite measurement systems.

- deduces the state of humidity of the soil below the surface using the data of humidity of the soil surface together with some physical parameters characteristic of the site in question.

(Manfreda et al., HESS-2014)

Vegetation Patterns